Charles University in Prague
Faculty of Science

Study Programme: Biochemistry
Study Branch: Biochemistry

Jindřich Durčák

Characterization of novel inhibitors of neuraminidase from influenza virus

Charakterisace nových inhibitorů neuraminidasy z chřipkového viru

Diploma thesis

Supervisor: doc. RNDr. Jan Konvalinka, CSc.

Prague 2015

Prohlašuji, že jsem tuto diplomovou práci vypracoval samostatně pod vedením školitele doc. RNDr. Jana Konvalinky, CSc. a všechny použité prameny jsem řádně citoval.

V Praze 7.5.2015 .....

Jindřich Durčák

Acknowledgements

First of all, I would like to thank my supervisor Jan Konvalinka for his kind leadership and many advices that he gave me. It was a pleasure to work in such a creative and positive work environment.

My great thanks also belong to Milan Kožíšek for countless professional suggestions, explanation of many methods and exemplary work attitude.

I thank Iva Flaisigová and Jana Starková for their support in laboratory, especially for excellent technical assistance with eukaryotic expression system.

My huge thanks belong to my family and girlfriend for great support throughout my studies.

Table of Contents

List of abbreviations

ACES	N–(2–Acetamido)–2–aminoethanesulfonic acid
APS	ammonium persulfate
BSA	bovine serum albumine
DMSO	dimethyl sulfoxide
DNA	deoxyribonucleic acid
dNTP	deoxynucleotide triphosphate
EDTA	ethylenediaminetetraacetic acid
FDA	Food and Drug Administration
HA	haemagglutinin
HABA	2–(4–hydroxyphenylazo)benzoic acid
HEPES	4–(2–hydroxyethyl)–1–piperazineethanesulfonic acid
HPLC	High – performance liquid chromatography
ICTV	International Committee on Taxonomy of Viruses
IOCB	Institute of Organic Chemistry and Biochemistry AS CR, v.v.i.
ITC	isothermal titration calorimetry
M1	matrix protein 1
M2	matrix protein 2
MES	2–(N–morpholino)ethanesulfonic acid
MOPS	3–(N–morpholino)propanesulfonic acid
MS	mass spectrometry
MUNANA	2'–(4–methylumbelliferyl)–D–N–acetylneuraminic acid
NA	neuraminidase
NANA	N–acetylneuraminic acid
NEP	nuclear export protein
NP	nucleoprotein

NS1	nonstructural protein 1
NS2	nonstructural protein 2
PA	acidic protein
PAGE	polyacrylamide gel electrophoresis
PB1	polymerase basic protein 1
PB2	polymerase basic protein 2
PCR	polymerase chain reaction
RDE	receptor destroying enzyme
RFU	relative fluorescence units
RNA	ribonucleic acid
RNP	ribonucleoprotein
RPM	revolutions per minute
SDS	sodium dodecyl sulfate
TEMED	tetramethylethylenediamine
WHO	World Health Organization

Abstract

Influenza virus causes common illness that annually infects several million people worldwide. Although the seasonal flu usually isn't life threatening, it is dangerous mainly for very young and elderly individuals. Nevertheless, a major threat for every person are new influenza strains that arise from a reassortment of viral strains that invade different species. Newly reassorted flu viruses have caused several pandemics with devastating effects, and so it is necessary to search for new treatment approaches that would prevent similar cases in future.

Influenza virus neuraminidase is a protein located on the surface of viral particles. It catalyzes the release of newly formed virions from cytoplasmic membrane of infected cells and plays a key role in the life cycle of influenza virus. As an enzyme with defined substrate, neuraminidase is a very good target for development of drugs, which would inhibit its function, and thus prevent further virus spreading.

By 2015, only four drugs against influenza were approved worldwide. Two of them, oseltamivir and zanamivir, target neuraminidase. Because of significant influenza resistance against the two remaining drugs (amantadine a rimantadine) occurred, neuraminidase inhibitors are virtually only medications. Therefore, development of new inhibitors becomes one of the main objectives of influenza virus research, also due to frequent incidence of drug – resistance among influenza strains.

One of the novel inhibitors is tamiphosphor. It is a oseltamivir derivative that was designed to create strong interactions with residues in neuraminidase binding site. Within this diploma thesis, characterization of binding of oseltamivir carboxylate and tamiphosphor was performed with neuraminidase from influenza virus subtype H7N9 that emerged in 2013 in China. Although this influenza strain has infected only a few hundred people, the disease mortality was nearly 40 %. Analysis of biomolecular interactions with inhibitors by isothermal titration calorimetry provides valuable information about complex formations and it can help in the development of new drugs.

Key words: neuraminidase; isothermal calorimetry; enzyme kinetics; recombinant proteins

Abstrakt

Virus chřipky způsobuje běžné onemocnění, které ročně prodělá několik milionů lidí na celém světě. Ačkoli sezónní chřipka většinou neohrožuje na životě, je nebezpečná především pro velmi mladé jedince a seniory. Velkou hrozbou jsou však nové kmeny chřipky, které vznikají kombinací chřipkových kmenů napadajících různé živočišné druhy. Takto vzniklé chřipkové viry již v minulosti způsobily několik pandemií s devastujícími účinky, a proto je nutné hledat nové možnosti léčby, které by v budoucnosti zabránily podobným případům.

Neuraminidasa chřipkového viru je protein nacházející se na povrchu virových částic, kde zajišťuje uvolnění nově vytvořených virionů z cytoplazmatické membrány napadených buněk a hraje tak klíčovou roli v životním cyklu chřipkového viru. Jakožto enzym s definovaným substrátem je neuraminidasa velmi dobrým cílem pro vývoj léčiv, které by inhibovaly její funkci a znemožnily tak další šíření viru.

Do roku 2015 byla celosvětově schválena pouze čtyři léčiva proti chřipce, z čehož dvě, oseltamivir a zanamivir, cílí právě neuraminidasu. Z důvodu značné rezistence chřipkových virů na zbylá dvě léčiva (amantadin a rimantadin) jsou inhibitory neuraminidasy v podstatě jedinými užívanými léky. Vývoj nových inhibitorů se proto stává jedním z hlavních cílů výzkumu chřipkového viru, i kvůli častému výskytu rezistence vůči již používaným lékům.

Jedním z nových inhibitorů je tamifosfor, derivát oseltamiviru, který byl navržen tak, aby vytvářel silné interakce ve vazebném místě neuraminidasy. V rámci této diplomové práce byla provedena charakterizace vazby inhibitorů oseltamivir karboxylátu a tamifosforu na neuraminidasu z chřipkového viru subtypu H7N9, který se objevil v roce 2013 v Číně. Přestože tento kmen chřipky nakazil pouze několik stovek lidí, mortalita onemocnění byla téměř 40 %. Analýza interakcí biomolekul s inhibitory pomocí isothermální titrační kalorimetrie přináší cenné informace o vzniku komplexů a může tak pomoci při vývoji nových léčiv.

Klíčová slova: neuraminidasa; isothermální kalorimetrie; enzymová kinetika; rekombinantní proteiny

1 Theoretical Part

Influenza virus is one of the most common infectious diseases of humans. Influenza occurs globally with an annual attack rate estimated at 5 % – 10 % in adults and 20 % – 30 % in children. Illnesses can result in hospitalization and death mainly among high – risk groups (the very young, elderly or chronically ill). Worldwide, these annual epidemics are estimated to result in about 3 to 5 million cases of severe illness, and about 250 000 to 500 000 deaths [1]. As a notorious case in point, the pandemic of 1918 – 1919 (Spanish flu) caused possibly 20 – 50 million deaths on a global scale, making it the most devastating disease outbreak in human history [2].

1.1 Influenza virus

Influenza viruses are single – stranded, negative – sense RNA viruses that cause regular seasonal epidemics in humans, other mammalian species and birds [3]. Three phylogenetically and antigenically distinct viral types – A, B and C – circulate globally in human populations, although type A viruses exhibit the greatest genetic diversity, infect the widest range of host species and cause the vast majority of severe disease in humans, including the great pandemics. The genome of Influenza A virus (total length $\sim$ 13 kb) is composed of eight segments that code viral proteins. Wild waterfowl are the reservoir hosts for type A influenza viruses, harbouring numerous antigenically distinct subtypes (serotypes) of the two main viral antigens – surface glycoproteins, the haemagglutinin (HA) and neuraminidase (NA) [4].

These avian viruses occasionally transmit to other species, in which they cause isolated outbreaks with little or no onward transmission. Less frequently, they become established in new hosts, resulting in (irregular) major human pandemics, for example the case with avian H5N1 influenza in humans that was a dangerous threat in 2004 [3].

1.1.1 Classification

Influenza is a RNA virus that belongs to the *Orthomyxoviridae* family (Group V of Baltimore classification). There are three genera of influenza virus: Influenzavirus A, Influenzavirus B and Influenzavirus C. Each genus includes only one species (or type): Influenza A virus, Influenza B virus, and Influenza C virus, respectively [5]. The three

genera of Influenzavirus are identified by antigenic differences in their nucleoprotein and matrix protein and they differ by target hosts:

- Influenzavirus A infects humans, other mammals, birds, and causes all pandemics
- Influenzavirus B infects mainly humans and also seals
- Influenzavirus C infects humans, dogs and pigs

Every strain of Influenzavirus is organized by International Committee on Taxonomy of Viruses (ICTV) using standard nomenclature [6]. An example of strain name is shown next:

A/swine/Missouri/2124514/2006

First of all the virus type is given, in this case Influenza A virus, next there is the organism, from which was virus isolated, however this information is omitted if virus was isolated from human. The geographical origin follows, then the strain number is given and on the last place is the year of isolation (2 – digit year if virus was isolated during the 1900s and 4 – digit year if virus was isolated in year 2000 or later).

Although every virus strain can be precisely designated by the name given by ICTV, most of the time (and also in news media) influenza viruses are described by viral subtype, e.g. H1N1, H3N2, H7N9. This description is determined by two glycoproteins on virions' surface – haemagglutinin and neuraminidase [7]. Depending on the sequence differences, there are already 16 HA subtypes and 9 NA subtypes defined [8]. Furthermore with discoveries of influenza virus in bats in South America, some of the resources state 18 HA subtypes and 11 NA subtypes [9, 10]. Even though many combinations of HA and NA subtypes were observed in nature, only H1, H2 and H3, and N1 and N2 subtypes are commonly found in humans [11]. And out of the 16 HA subtypes, the H2, H5, H6, H7 and H9 viruses are considered to have pandemic potential [12].

1.1.2 Influenza pandemic

Due to the fact that influenza symptoms could be caused by different illnesses, it is hard to determine when was the first time that influenza virus occurred. First symptoms of influenza were described roughly 400 years Before Christ and pandemics of influenza have been reported since the early sixteenth century, but the first laboratory diagnosis of influenza was performed in 1932 [13, 14, 15].

1.1.2.1 1918 Spanish flu

The most severe attack of influenza pandemic occurred in years 1918 – 1919 [16]. During the first wave of disease outbreak, wartime censors minimized early reports of illness and mortality in Germany, Britain, France, and the United States to maintain morale. However news media were free to report the epidemic's effects in neutral Spain, creating a false impression of Spain as especially hard hit or origin of infection, thus the pandemic got it's nickname – Spanish flu (strain name A/Brevig Mission/1/18). This H1N1 viral subtype caused acute illness in 25 % – 30 % of the world's population and spread all over the globe even to the Arctic and remote Pacific Islands [17]. The disease was also exceptional with mortality rates among the infected of over 2.5 %, as compared with less than 0.1 % in other influenza epidemics. Symptoms were so unusual that initially influenza was misdiagnosed as dengue, cholera, or typhoid. One of the most striking complications was hemorrhage from mucous membranes, especially from the nose, stomach, and intestine. Bleeding from the ears and petechial hemorrhages in the skin also occurred. The majority of individuals who died during the pandemic succumbed to secondary bacterial pneumonia (and respiratory failure), since no antibiotics were available in 1918. The virus also killed people directly, causing massive hemorrhages and edema in the lungs [18]. Furthermore, most death emerged among young adults, a group that usually has a very low death rate from influenza (Figure 1 on the following page).

The total mortality of Spanish flu is not known, but it is estimated that 2 % to 5 % (20 – 50 million people) of the world's population was killed. As many as 25 million may have been killed in the first 25 weeks, in contrast, HIV/AIDS has killed 25 million people in its first 25 years [19].

1.1.2.2 1957 Asian flu, 1968 Hong Kong flu

Then, in February 1957, a new influenza virus suddenly appeared in Southeast China and it subsequently spread to countries worldwide [20]. This type Influenza A virus, subtype H2N2, caused the "Asian flu" (strain name A/Singapore/1/1957) pandemic during which H1N1 strains disappeared completely from the human population. In total, the pandemic affected some 40 % – 50 % of people, of which 25 % – 30 % experienced clinical disease [21]. The course of infection was clinically typical, with most deaths due to secondary bacterial pneumonia. The mortality rate was estimated at approximately 0.1 %

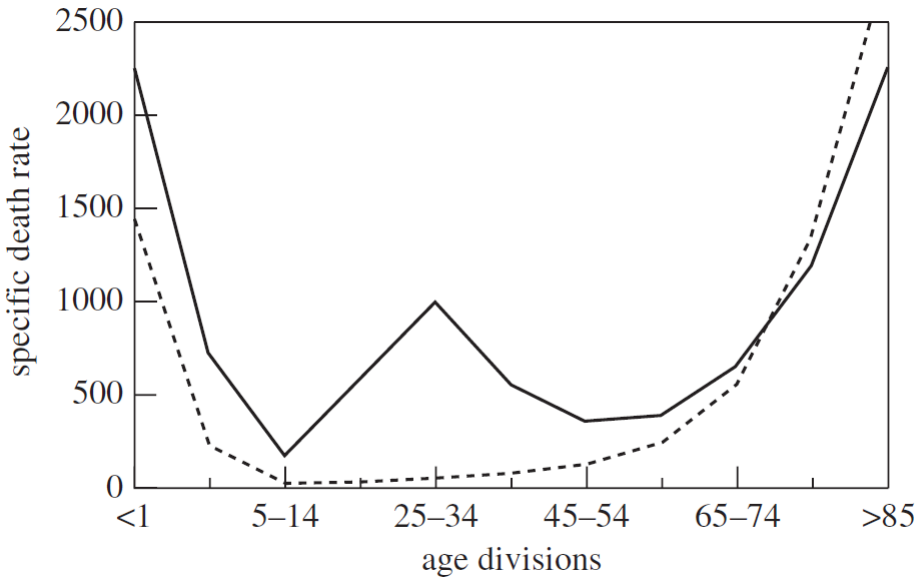

Figure 1: Influenza and pneumonia mortality by age in the USA. Average of interpandemic years 1911 – 1915 (dashed line) and pandemic year 1918 (solid line). The specific death rate is per 100 000 of population in each age division. Reproduced from [17].

– 0.2 % (1 000 000 – 2 000 000 deaths), predominantly in the very young and very old people.

Asian (H2N2) influenza persisted until 1968, when another new virus suddenly appeared in China [20]. This virus, subtype H3N2, descended from H2N2 by antigenic shift (see section 1.1.4.4 on page 21 for detailed explanation), in which genes from multiple subtypes reassorted to form a new virus and caused the pandemic which is known as "Hong Kong flu" (A/Hong Kong/1/68) during which H2N2 subtype viruses disappeared completely from people. It is thought to have caused around 1 million deaths worldwide with mortality rate lower than 0.1 %.

1.1.2.3 Pandemics since 1970s

Strictly speaking, there was a fourth pandemic in the 20th century, an H1N1 strain which appeared in 1977 – Russian flu (sometimes called red flu; A/USSR/90/77). This was a "benign" pandemic, almost entirely restricted to persons born after year 1950, because the older population had protective immunity resulting from prior experience with H1N1 strains, which were almost identical. Therefore some sources assume that this virus was kept frozen in a yet unidentified laboratory from 1950s and then it was accidentally released

[22, 23]. Nevertheless Russian flu had no fatal effect on population, not exceeding annual influenza epidemics.

So far in the 21st century influenza pandemic occurred once. In 2009, the pandemic Influenza A virus infection (H1N1 strain, also called "swine flu"; A/Mexico/InDRE4487/2009 or A/California/07/2009). After the virus was observed for the first time, it appeared to be a reassortment of human, avian and swine flu in swine, leading to creation of entirely new viral strain. It was the third time (including Russian flu) that pandemics were involving H1N1 influenza virus (the first of them being the Spanish flu pandemic), however in a new version. Although news media paid a lot of attention to swine flu, the pandemics were not nearly as devastating as previous pandemics, but still causing more than 18.000 deaths and were associated with more than 200.000 estimated respiratory deaths worldwide [24, 25].

The interval of time between pandemics varies from a decade (1957 to 1968) to almost 50 years (1918 to 1957). These intervals have not significantly increased or decreased with the passage of time, suggesting that increasing population and travel are not determining factors [21]. Although infections in humans with avian strains are uncommon, several outbreaks of severe influenza with highly virulent strains derived from infected poultry were reported in China and other Asian countries since 2003 (last case was reported in 2013 with H7N9 influenza subtype) and avian strains still represent a very dangerous threat. The recent uncertainty whether H5N1 avian influenza virus will adapt to human transmission, and how its spread might be controlled, highlight the threat that is posed by influenza and the need to understand its evolutionary dynamics [26, 27].

1.1.3 Structure of influenza virus

All three genera of of influenza viruses (Influenzavirus A, Influenzavirus B and Influenzavirus C) are very similar in overall structure [28]. By electron microscopy, influenza A and B viruses are virtually indistinguishable. They are spherical or filamentous in shape, with the spherical forms on the order of 100 nm in diameter and the filamentous forms often in excess of 300 nm in length. Influenza C virions are structurally distinct from those of the A and B viruses and also contain only seven genomic segments (one segment less than influenza A and B viruses). They can form long cord – like structures on the order of 500 μm on infected cell surfaces. However, influenza C virions are compositionally

similar, with a lipid envelope overlying a protein matrix and the ribonucleoprotein (RNP) complex studded with glycoproteins.

1.1.3.1 Influenza genome

The genome of Influenza A virus is composed of eight genomic segments of negative – sense RNA (total length $\sim$ 13 kb) that, by convention, are listed from largest to smallest, although their true arrangement within the spherical virion is unknown [3]. Each segment contains a coding region that encodes one or two proteins, as well as short 5' and 3' flanking sequences. Three segments encode proteins that form the viral polymerase complex – polymerase basic protein 1 (PB1; approximately 2 300 nucleotides in the protein – coding region), polymerase basic protein 2 (PB2; $\sim$ 2 300 nucleotides) and acidic protein (PA; $\sim$ 2 150 nucleotides). Two segments encode surface envelope glycoproteins that function as viral antigens – haemagglutinin (HA; $\sim$ 1 700 nucleotides) and neuraminidase (NA; $\sim$ 1 400 nucleotides). A single segment encodes a nucleoprotein (NP; $\sim$ 1 500 nucleotides). The seventh segment encodes two proteins that share a short overlapping region – the matrix protein (M1; $\sim$ 750 nucleotides) and M2 proton channel ($\sim$ 300 nucleotides). Segment 8, the smallest segment of the viral genome, encodes a nonstructural protein 1 (NS1; $\sim$ 700 nucleotides) and also with an overlapping reading frame encodes the nonstructural protein 2 (NS2; $\sim$ 350 nucleotides), sometimes also called nuclear export protein (NEP). A mature virion of Influenza A virus is composed of the nucleoprotein, a surrounding layer of M1 protein, and the membrane envelope, which contains the HA, NA and M2 proteins. The structure of Influenza A virus is shown in Figure 2 on the following page.

1.1.3.2 Influenza proteins

On the surface of influenza viruses, there are two large glycoproteins – haemagglutinin and neuraminidase (function and properties of neuraminidase are described in section 1.2 on page 24). Haemagglutinin attaches the viral particle to terminal sialic acids on the host cell surface for viral entry and promotes the release of viral ribonucleoprotein complexes through membrane fusion [29]. HA is a trimer, commonly divided into a head region and a stem region. Each chain is synthesized as a precursor polypeptide and then cleaved by host cell proteases into two fragments, HA1 ($\sim$ 330 amino acids) and HA2 ($\sim$ 220 amino acids), linked by a disulfide bond. Both roles of HA in the viral life cycle have been

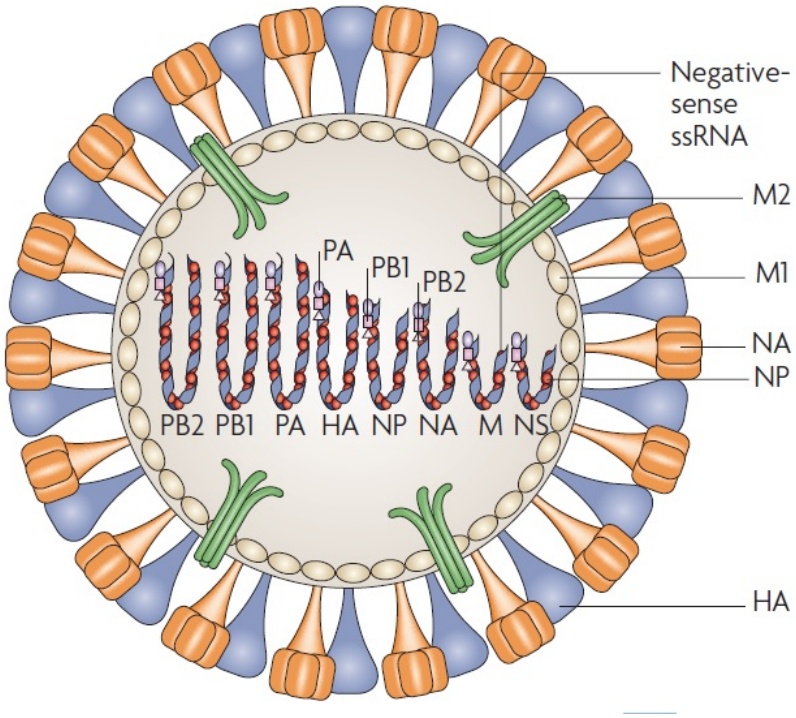

Figure 2: The structure of Influenza A virus. Detailed description is provided in text. Reproduced from [3].

targeted for therapeutic design. The receptor binding site is in the head region, lined by three structural elements of HA1 within each monomer, including the 190 – helix, the 130 – loop and the 220 – loop [30]. Binding of small molecules such as tert – butylhydroquinone to HA was found to inhibit membrane fusion and led pharmaceutical companies to search novel inhibitors of HA, but so far no new compound has been accepted for influenza clinical treatment [31].

The main function of nucleoprotein is to encapsidate the segmented viral RNA and to bind with the three polymerase subunits, PA, PB1 and PB2, to form ribonucleoprotein particles for RNA transcription, replication and packaging [32]. In each ribonucleoprotein particle, the viral RNA wraps around individual NP molecules, which are strung together by burying the "tail loop" (residues 402 – 428) of one NP molecule inside an adjacent NP molecule. Newly assembled RNP particles bound with the M1 protein are then exported from the host cell nucleus.

Matrix protein 1 forms an intermediate layer between the membrane bound HA, NA and M2 proteins and the eight ribonucleoprotein segments [33]. In the nucleus of infected

cells, binding of M1 to newly assembled RNP particles is essential for their export and later it is also the major driving force in virus budding. M2 protein forms a tetrameric proton – selective ion channel activated by the low pH of endosomes. Each M2 monomer has only approximately 100 residues. The N – terminal 25 residues are exterior to the viral membrane, followed by a single transmembrane helix and amphipathic helix residing at the hydrophobic – hydrophilic interface of the viral membrane inner layer [34]. The final 35 residues of C – terminal are in the viral interior.

Nonstructural protein 1 protects influenza viruses against the antiviral responses mediated by interferon α/β in infected cells [35]. NS1 consists of 230 or 237 residues (number differs by strain) and forms a dimer. It has two functional domains – N – terminal domain (residues 1 – 73) that binds double – stranded RNA and C – terminal domain (residues 74 – 230/237) that binds multiple cellular proteins that are required for the processing of all cellular pre – mRNAs. Nonstructural protein 2 mediates the export of newly synthesized ribonucleoprotein particles from the nucleus of infected cells and as such, it is also referred to as the nuclear export protein [36].

The last three proteins – polymerase basic protein 1, polymerase basic protein 2 and acidic protein serve as subunits that form heterotrimeric RNA – dependent RNA polymerase [28]. After virus reaches the nucleus of the host cell, the RNA polymerase (as part of an ribonucleoprotein) first transcribes and then replicates the viral RNA. The newly synthesized viral mRNA has a 5' – capped fragment cleaved from host pre – mRNA. The fragment is cleaved by N – terminal domain of acidic protein that possess endonuclease activity. The C – terminal domain harbors a "mouth" where N – terminal region (residues 1 – 16) of PB1 is inserted. PB1 contains the polymerase domain, but neither the structure nor the precise boundary of this domain is known. The C – terminal region (residues 678 – 757) of PB1 complexes with the N – terminal region (residues 1 – 37) of PB2. Subunit PB2 is believed to contain RNA binding domain [37, 38, 39].

1.1.4 Influenza virus life cycle

The life cycle of influenza viruses has been studied in detail and almost all the viral proteins are becoming potential therapeutic targets [40]. Influenza life cycle (shown in Figure 3 on the following page) involves virion attachment and entry, viral RNA synthesis and protein production, assembly, budding and release of new infectious virions.

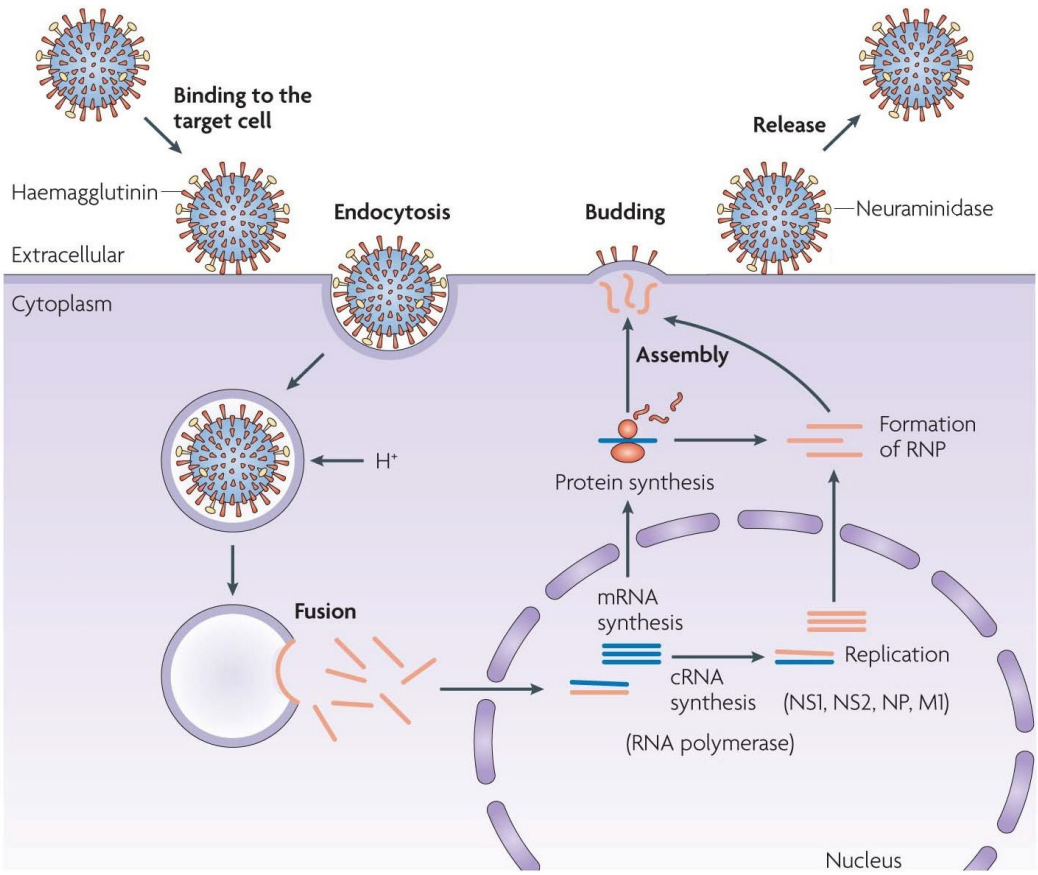

Figure 3: Influenza virus life cycle. Detailed description is provided in text. Reproduced from [41].

1.1.4.1 Virus attachment and entry

Haemagglutinin on influenza virus surface recognize N – acetylneuraminic acid (NANA; also called sialic acid) on the host cell surface [28]. N – acetylneuraminic acids are nine carbon acidic monosaccharides that are usually found at the termini of many common glycoconjugates that occur in various cell types and animal species. During virus replication in influenza life cycle, haemagglutinin is cleaved by serine proteases into two subunits HA1 and HA2. This post – translational modification is crucial for virus attachment and infectivity [42]. The HA1 portion contains the receptor binding and antigenic sites, while the HA2 subunit is thought to mediate the fusion of viral envelope with host cell membranes. Virus infectivity could be neutralized by antibodies that bind to haemagglutinin, so individual viral strains evolve frequent amino acid changes at the antigenic sites. On the other hand the structural configuration of HA is conserved among strains and subtypes.

After mutations in many antigenic sites accumulate, such virus strain isn't neutralized by host antibodies to the original strain, and the infected organism are susceptible against so – called drifted strain.

After haemagglutinin successfully attaches to terminal sialic acid of host cell, virus is endocytosed [43]. The crucial physical property in viral particle uncoating is the endosomal compartment acidity, which affects this process in two ways. Firstly, low pH of endosomal compartment triggers conformational change in haemagglutinin that exposes a fusion peptide. This peptide mediates viral membrane merging with membrane of endosomal compartment, thus opening a membrane pore through which viral ribonucleoprotein particles enter infected cell cytoplasm [44]. Secondly, hydrogen ions from endosomal compartment are pumped into virions via the M2 ion channel. This channel, which occurs only in Influenzavirus A, has external region on surface of viral particles and decreases viral particle pH that disrupts protein – protein interactions, therefore allowing ribonucleoprotein particles to be released from viral matrix into host cell cytoplasm.

1.1.4.2 Viral RNA synthesis and protein production

Following release from virions, ribonucleoprotein particles are transported to infected cell nucleus, using viral proteins' nuclear localization signals that direct host cell proteins to transport viral RNP and other viral proteins into cell nucleus [45]. Host cell nucleus is the site of all influenza virus RNA synthesis – both mRNA that is used for viral protein translation and viral RNA that serves as genome for new viral particles. The viral RNA – dependent RNA polymerase that is being transported into host cell nucleus as part of RNP, uses viral negative – sense RNA as a template to synthesize both messenger RNA for protein production and complementary RNA intermediates that are subsequently transcribed again by viral RNA polymerase for more copies of negative – sense, genomic influenza RNA.

Influenza messenger RNA is then exported from host cell nucleus and it can be translated just like cellular mRNA [28]. On the other hand the export of viral RNA segments that will form influenza genome, is mediated by viral proteins M1 and NS2. Matrix protein 1 interacts both with viral RNA segments and nucleoprotein, therefore it is thought to participate in formation of ribonucleoprotein complex. Matrix protein 1 also associates with nonstructural protein 2, which mediates M1 – RNP export from nucleus to cytoplasm via

nucleoporins. The envelope proteins haemagglutinin, neuraminidase and M2 ion channel are synthesized in endoplasmic reticulum membrane – bound ribosomes, proteins are then folded and transported to Golgi apparatus, where post – translational modification takes place. Apart of envelope proteins, only little is known about translation and transport of the remaining viral proteins [46].

1.1.4.3 Virus assembly, budding and release

Influenza viral particles are not fully infectious until they contain full genome of eight segments. Formerly it was believed that viral RNA packaging is a random process and only particles that end up with whole genome can be released from host cell, but recent research suggests that packaging is strictly controlled process, during which individual genome segments are assembled to form particles with complete genome that are transported to cell membrane [47].

Budding of influenza virus is probably initiated by matrix protein 1 accumulation at intracellular part of cell membrane, after which all influenza virus components start to form new virions. After budding is complete, haemagglutinin still binds virions to the sialic acid on host cell surface. Virus progeny is finally released when neuraminidase cleaves terminal sialic acid from cell surface glycoproteins. Neuraminidase also removes sialic acid from virus envelope, preventing haemagglutinin from binding sialic acid of another virion that would cause aggregation and decreased infectivity. This crucial role in viral life cycle makes neuraminidase a promising target for anti – influenza drug design [28].

1.1.4.4 Antigenicity

Antigenicity is the ability of a antigen to react specifically with the functional binding site of a complementary antibody [48]. In case of influenza virus, there are two major processes that determine influenza health impact – antigenic drift and antigenic shift. These two processes are the key factors why influenza is a classic example of reemerging virus that cause annual epidemics and occasional worldwide pandemics at unpredictable intervals [36].

1.1.4.4.1 Antigenic drift

Due to viral error – prone RNA – dependent RNA polymerase, the influenza virus

is subject to rapid mutation, especially surface glycoproteins haemagglutinin and neuraminidase, against which immunity response of infected organism is directed, and serum antibody to haemagglutinin is the most important factor in immunity [49]. The progressive accumulation of mutations over years in the viral genome is called antigenic drift. For haemagglutinin, the rates of evolution are approximate 6.7×10^{-3} substitutions per nucleotide per year and for neuraminidase, 3.2×10^{-3} substitutions per nucleotide per year [50]. Because of these mutations, the modified viruses can't be inhibited well by antibodies against original strains and virus can also spread throughout population more easily. In haemagglutinin most of mutation occur in the HA1 binding domain as a result of immune selection. The genetic drift of viral surface glycoproteins demands constant surveillance, so that antigenicity of circulating strains will be studied and influenza vaccines can be updated when necessary.

1.1.4.4.2 Antigenic shift

Antigenic shift (or reassortment), seen only with Influenza A virus, is another process, during which whole genome segments are replaced by corresponding segments from another influenza strain [28]. This reassortment occurs in cells that are infected by different species of influenza viruses. Usually the source of newly inserted segments is large reservoir of influenza viruses in waterfowl. The most commonly shifted segments are haemagglutinin and neuraminidase, which results in novel influenza subtypes with new antigenic proteins that have not been observed in human, thus with no preexisting immunity [51]. The outcome of new shifted haemagglutinin (and neuraminidase) in human viruses is usually a global pandemic, caused by a virus to which humans are susceptible, but immunologically naive. Well described case is the 2009 pandemics (swine flu), when avian, human and swine influenza virus reassorted in swine, resulting in a new virus [52].

1.1.4.5 Influenza disease and treatment Influenza (often simplified as flu) is a contagious respiratory viral illness with worldwide appearance [53]. Influenza infects humans independently on age or gender with usual course of the disease without fatal consequences – fever, cough, pains, stomachaches, headaches, fatigue and overall weakness. However there are certain groups of people that are at higher health risk, especially older people, young children and individuals with chronic cardiac, renal and respiratory diseases.

Mainly in these groups complications of influenza might occur, including secondary bacterial pneumonia, post – influenza encephalitis and various secondary bacterial infections. It is also believed that seriousness of influenza infection is determined by the location where virus attaches in host organism [54]. The influenza strains that are easily transmitted between humans, bind to receptors in upper part of the respiratory tract (mouth, nose, throat) and cause regular course of infection, while influenza strains that predominantly bind to receptors deep in lungs cause severe viral pneumonia and high lethality (for example strain H5N1 from year 2004 that caused so – called "bird flu"). Nevertheless strains with receptors deep in lungs are not as easily transmitted by coughing and sneezing. Current approach to fighting influenza could be divided to vaccines and classic treatment with antivirotic compounds.

1.1.4.5.1 Influenza vaccines

The optimal approach to preventing influenza illness and its potentially dangerous complications is vaccination [55]. Influenza vaccine usually consists of three or sometimes four influenza strains that are chemically "inactivated". Recent seasonal flu epidemics are dominated by the H3N2 and H1N1 subtypes (along with influenza B viruses), therefore vaccines contain one H1N1 subtype strain, one H3N2 subtype strain and one influenza type B strain. Individual vaccine components are varied every year in the hope of matching the upcoming viral strains in the next flu season [33].

The immunogenicity of vaccines is directly correlated to haemagglutinin immunoglobulin G levels following vaccination [56]. After binding to HA these antibodies inhibit the attachment of viral particles to its receptors on respiratory cells and overall concentration of anti – HA antibodies determine whether the vaccine recipient will be protected from influenza infection or will experience decreased disease severity [57].

1.1.4.5.2 Influenza antivirotics

Worldwide there are currently four clinically approved compounds for influenza treatment – two adamantane derivatives that target M2 ion channel, amantadine and rimantadine, and two neuraminidase inhibitors, oseltamivir (Tamiflu®) and zanamivir (Relenza®) [58]. Neuraminidase inhibitors are described in section 1.3 on page 28.

Amantadine and rimantadine act as channel blockers, binding to a transmembrane

region in the M2 proton channel where several drug – resistant mutations occur [34]. The resistance of influenza A viruses to amantadine or rimantadine can occur spontaneously or emerge rapidly during treatment. High incidence of drug – resistant mutations that occurred after treatment with these inhibitors has led the Centers for Disease Control and Prevention to recommend that these drugs should not be used [59].

1.2 Viral neuraminidase

The story of influenza neuraminidase started in the 1940s, almost ten years after the first influenza virus was isolated from human [7]. During an experiment by George Hirst from Rockefeller Institute in New York City in 1942, when allantoic fluid from embryonated chicken eggs, which had been infected with influenza virus, was mixed at 4°C with erythrocytes, the cells distinctly agglutinated. After these agglutinated cell were warmed to 37°C, they dispersed as the virus eluted and cells could not be reagglutinated when mixed with freshly infected allantoic fluid at 4°C. However the eluted virus agglutinated fresh red blood cells at 4°C, which led Hirst to his interpretation that the virus had an enzyme which removed receptors from agglutinated erythrocytes, which were binding viral particles after warmed to 37°C, where this enzyme was more active. Due to its function, the enzyme was first called receptor destroying enzyme (RDE).

Later it was suggested that receptor destroying enzyme might yield a "split product" [60]. Eventually this product was isolated and characterized as N – acetylneuraminic acid (sialic acid), and RDE became known as neuraminidase or sialidase. This discovery was the key feature in structure based drug design in future.

Neuraminidase is a glycoside hydrolase enzyme (EC 3.2.1.18) that cleaves glycosidic linkages of neuraminic acids. During budding of virus progeny on infected cells surface, neuraminidase cleaves terminal sialic acid from cell's glycoproteins, allowing novel viral particles to leave host cell instead of binding to sialic acid via haemagglutinin. After virions are released, neuraminidase also cleaves terminal sialic acids from virions' surface, preventing the virus from coagulation. Furthermore neuraminidase is thought to increase virus infectivity by breaking down mucins in respiratory tract of infected organisms, which supports the virus in penetration to the respiratory epithelium [61, 62].

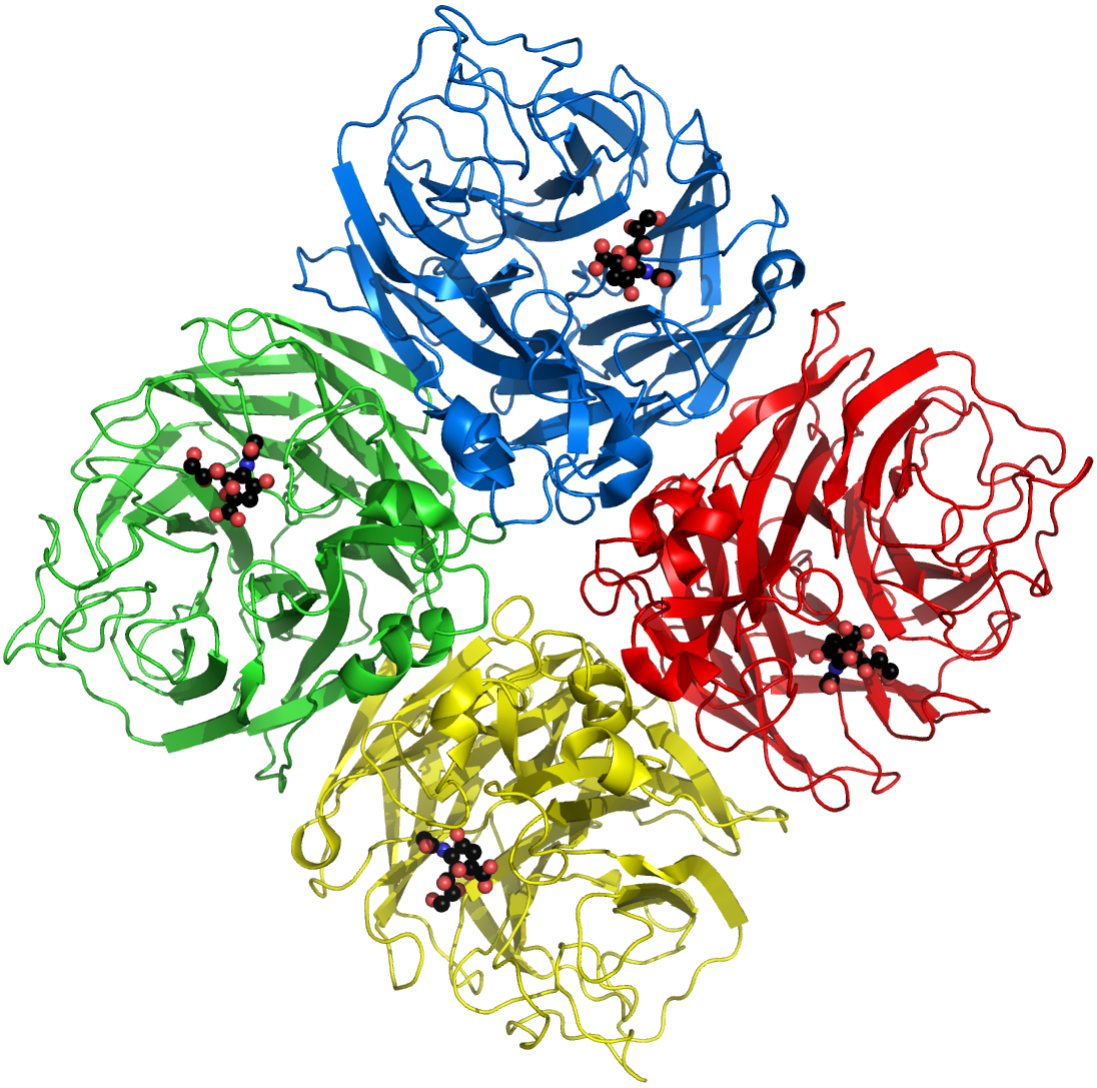

Figure 4: Neuraminidase tetramer from influenza virus. Individual monomers are pictured in different colors. Sialic acids bound in each neuraminidase monomer active site are in sphere representation. The image was created by computer program PyMOL from pdb file 1W21 [63].

1.2.1 Neuraminidase structure

Viral neuraminidase is a tetramer that is composed of four identical monomers, each of which contains a single polypetide chain coded by sixth RNA segment from influenza genome [60]. Neuraminidase is anchored in the viral membrane lipid bilayer by hydrophobic amino acids that are predicted to form transmembrane helix near the N – terminal end of neuraminidase sequence, which is followed by a stalk region that varies in it's length

and has unknown structure. All NA stalks contain predicted one to four sites of N – linked glycosylation, depending on the stalk length [64]. The majority of neuraminidase (called head; $\sim$ 380 amino acids) is on the surface of virions. The neuraminidase head sequence contains four N – glycosylation sites, each mediated by asparagine. Neuraminidase polypeptide doesn't undergo post – translational cleavage, no signal peptide is cut off and even initiating methionine is retained.

First neuraminidase structure was solved in 1978, when neuraminidase heads from several H2N2 and H3N2 influenza strains were released by pronase (mixture of proteases from *Streptomyces griseus*) and crystallized [65]. The neuraminidase structure shows that each NA monomer is composed of six topologically identical antiparallel β sheets that are organised in propellor conformation. The NA tetramer has 4 – fold circular symmetry and is stabilized by metal ions that are bound on the symmetry axis. Neuraminidase tetramer is shown in Figure 4 on the preceding page.

1.2.2 Catalytic site

There are four catalytic sites in NA head region (one catalytic site in each NA monomer), located in deep pockets that occur on the upper corners of the tetramer [60]. Although individual neuraminidase sequences differ by as much as 75 %, there are charged amino acids among the polypeptide that are conserved across all influenza strains. Based on N2 numbering these residues include Arg 118, Glu 119, Asp 151, Arg 152, Asp 198, Arg 224, Glu 227, Asp 243, His 274, Glu 276, Glu 277, Arg 292, Asp 330, Lys 350, Tyr 406 and Glu 425. During polypeptide folding, these conserved amino acids all come together and form the pocket that contains active site. This observation leads researchers to design novel inhibitors which would target conserved residues that are present in all strains and so, such drugs would possibly block catalytic sites of influenza strains that have not yet been found in human.

Enzymatic mechanism of viral neuraminidase appears to proceed via the formation of a sialosyl cation intermediate [41]. Firstly, sialic acid as the terminal monosaccharide of saccharide chain undergoes structural change from chair conformation to boat conformation and under the effect of general acid (Glu 277), terminal sialic acid is cleaved and forms sialosyl cation in half – chair conformation (positively charged oxygen forms a double bond). Then general base (Asp 151) deprotonates Tyr 406, which attacks sialosyl

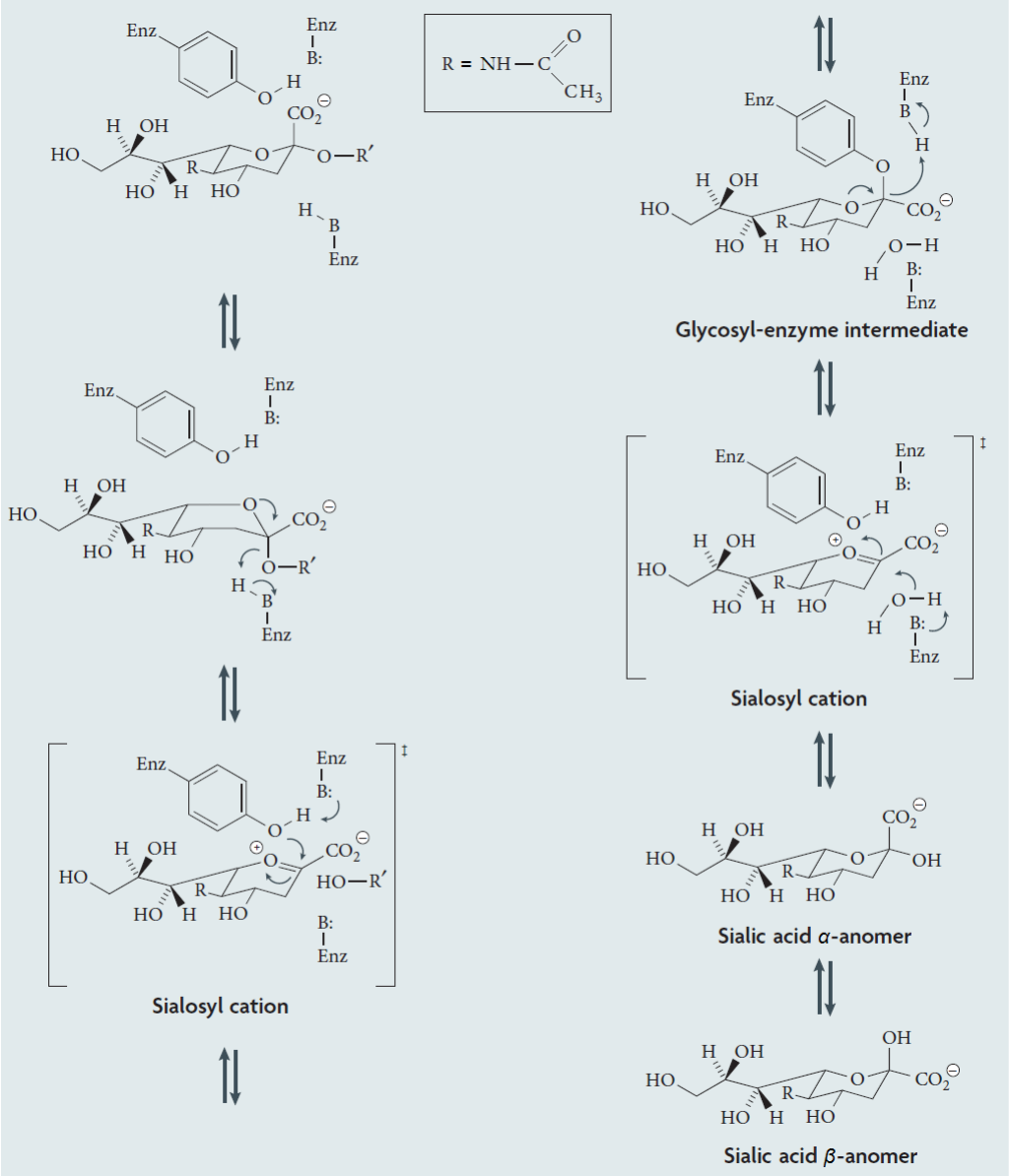

Figure 5: Enzymatic mechanism of influenza neuraminidase. R' represents carbohydrate chain, Enz represents enzyme, B: represents general base, $B—H$ represents general acid. Description of mechanism is provided in text. Reproduced from [41].

cation as nucleophile, a covalent bond is created and glycosyl – enzyme intermediate is formed. Regeneration step follows as sialosyl cation is produced again, while Tyr 406 and Asp 151 return to their original states. Water molecule then loses a proton to Glu 277, which becomes general acid again and hydroxide anion attacks sialosyl cation, which leads to creation of α – anomer of sialic acid that eventually mutarotates to the thermodynami-

cally more favorable β – anomer. Whole mechanism is showed in Figure 5 on the previous page.

1.2.3 Subtype comparison

By neuraminidase primary sequences, nine NA subtypes are classified into two groups. Group 1 contains subtypes N1, N4, N5 and N8, and group 2 comprises subtypes N2, N3, N6, N7 and N9 [64]. With crystallization and structure characterization of the last NA subtype (N7) that was done in 2014, every neuraminidase subtype has at least one solved structure [66]. Despite individual amino acid sequences have up to 75 % differences, overall topology of influenza neuraminidases is similar. On the other hand, both NA groups have little nuances in catalytic site structure. All group 1 uncomplexed neuraminidases have a 150 – cavity in the active site (with the exception of pandemic N1 from 2009 swine flu, although mutant I222R of this neuraminidase prepared by reverse genetics method contains the cavity) and all group 2 uncomplexed structures have no 150 – cavity. Furthermore subtypes N6 and N7 also contain a unique small cavity adjacent to the active site, named the 340 – cavity. Catalytic site comparison of all subtypes is showed in Figure 6 on the following page.

1.3 Neuraminidase inhibitors

Even though all influenza proteins have become potential targets when designing anti – influenza drugs, the most successful structure based drug design has arisen from targeting the neuraminidase. Therefore the functional and structural characterization of neuraminidase is beyond any importance for the control, treatment and prevention of influenza infections. If neuraminidase in viruses is absent, inactive or inhibited, viral particles clump together on host cells and infectivity is decreased. Furthermore NA inhibitors are nowadays the only class of antivirals that are effective in treatment of both Influenza A and B viruses, since most strains have resistance against M2 proton channel inhibitors, adamantanes, and only Influenza A virus has M2 protein [28, 41, 66].

Discovery that sialic acid is the product of neuraminidase action led to the development of inhibitors based on sialic acid structure. Since 1999 two neuraminidase inhibitors based on sialic acid structure have been licensed worldwide, oseltamivir (Tamiflu®) and

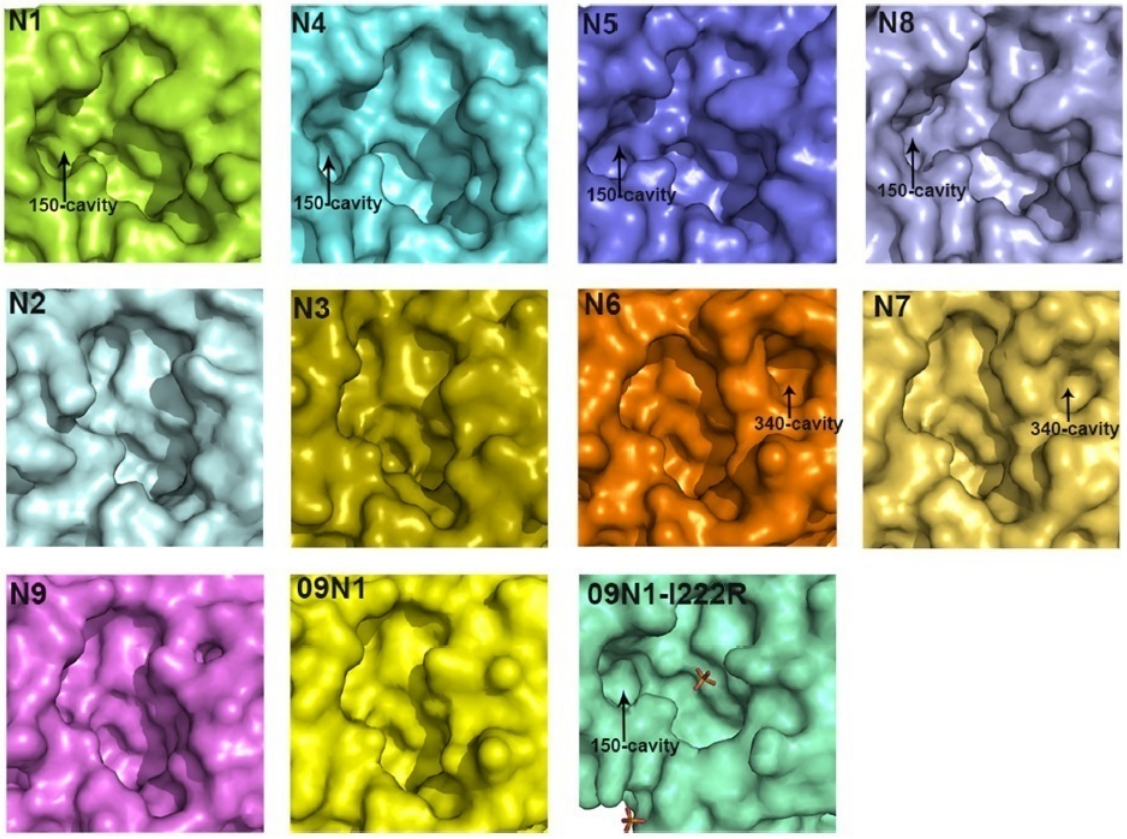

Figure 6: Catalytic sites from all Influenza A virus subtypes. Reproduced from [66].

zanamivir (Relenza®) [67]. In 2010 two new inhibitors were licensed in Japan, peramivir (Rapiacta®) and laninamivir (Inavir®). Peramivir has been licensed also in South Korea, and most recently in China as a response to growing concerns of Influenza A virus strain H7N9. Due to rapid emergence of drug – resistant influenza strains during treatment with antivirotics and the fact that vaccination is not a realistic strategy for prevention of rapidly spreading influenza pandemic, it is urgent to develop new anti – influenza drugs [33].

1.3.1 Oseltamivir and zanamivir

Oseltamivir and zanamivir were among the first examples of successful effort in structure – based drug design [33]. Inspired by the structure of sialic acid and the catalytic mechanism, researchers' initial focus aimed to sialic acid derivatives and sialosyl cation –

like compounds. It was thought that such molecules would not be quickly metabolized, but still should be recognized by viral neuraminidase. Sialic acid, sialosyl cation, zanamivir and oseltamivir are shown in Figure 7.

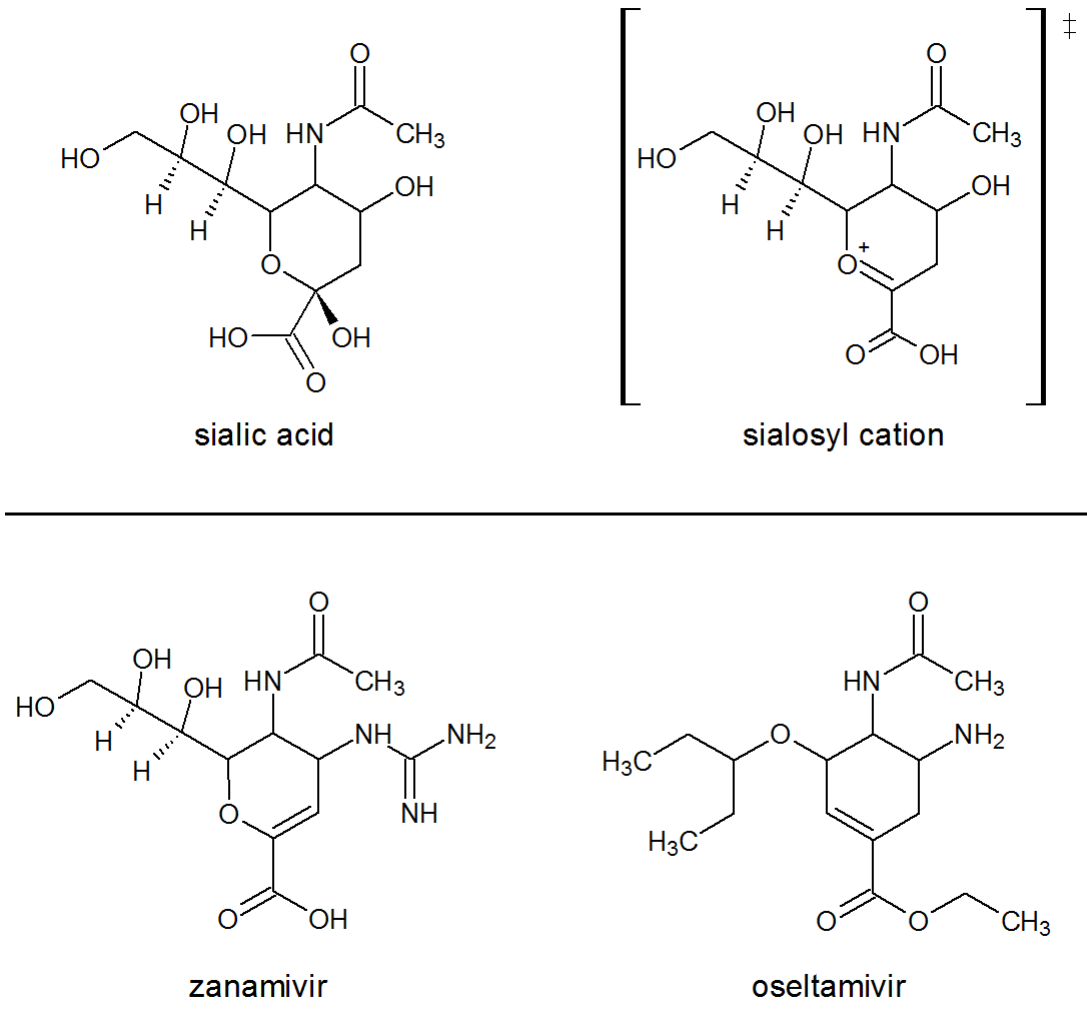

Figure 7: Sialic acid, sialosyl cation (intermediate of enzyme reaction), first approved neuraminidase inhibitors, zanamivir and oseltamivir. Chemical formulas were created by computer program ChemSketch.

After synthesis and testing of many compounds, the most potent inhibitor was selected as the lead drug candidate by Glaxo under name zanamivir and was approved by Food and Drug Administration (FDA) in 1999 as the first neuraminidase – targeting and also anti – influenza drug. By that time it had the highest affinity towards neuraminidase ($K_i = 2.0 \times 10^{-10}$ M) and it successfully stopped virus from forming new virions [41, 68].

Zanamivir has limited oral bioavailability due to its high polarity and fast excretion. Instead it was developed as an inhaled formulation, which delivers the drug straight to the site of infection.

Discovery of zanamivir was essential in further development of novel neuraminidase inhibitors. After significant progress that has been done in structure – activity relationship studies with N – acetylneuraminic acid derivatives and development of novel neuraminidase inhibitors that are based on non – carbohydrate templates such as cyclohexenes, a new inhibitor was discovered, labeled GS 4071 (known as oseltamivir carboxylate) [69]. Based on the previous mechanistic studies, the double bond in oseltamivir was positioned to more closely mimic the putative transition state of reaction intermediate – sialosyl cation. Also replacing the glycerol moiety from zanamivir with lipophilic 3 – pentyl ether side chain enhanced the affinity towards neuraminidase ($K_i = 1.7 \times 10^{-11}$ M) [70]. Although it had been hoped that compound GS 4071 might have had sufficient oral bioavailability, levels after oral intake were too low and so a prodrug strategy had to be chosen. Oseltamivir is the ethyl ester prodrug of GS 4071 that is converted to the active form *in vivo* by the action of endogenous esterases.

Both zanamivir and oseltamivir are effective against group 1 and group 2 neuraminidases. However active site structure determination and comparison of all subtypes that is in Figure 6 on page 29 shows that contrary to group 2 neuraminidases, 150 – cavity of group 1 enzymes adopts an open conformation, which opens a cavity next to the active site [33]. Therefore the 150 – cavity provides opportunities for designing inhibitors that would be selective and with increased affinity toward neuraminidases from group 1.

1.3.2 Laninamivir and peramivir

Even though novel neuraminidase inhibitors were discovered in early 2000s, there were no approved compounds for clinical treatment until 2010, when laninamivir and peramivir were licensed for use in certain part of world after emergence of drug – resistant influenza strains and global pandemics threat in 2009 [67]. Laninamivir and peramivir are shown in Figure 8 on the next page.

Laninamivir is very similar to zanamivir, it only differs in one methyl group that is added in side chain of laninamivir, creating methyl ether [71]. Laninamivir is administered as a prodrug, laninamivir octanoate, by inhalation in a powdered form and this derivative

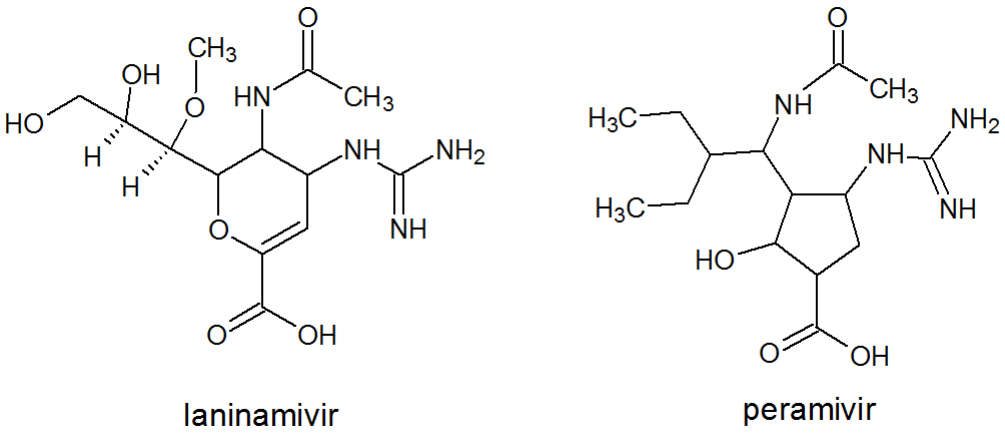

Figure 8: Laninamivir and peramivir. Chemical formulas were created by computer program ChemSketch.

is quickly converted into the active form in patient's lungs. The active form is retained in target tissues for a prolonged period of time (biological half – life is 41.4 hours; in some studies even 3 days compared to 2.5 hours of biological half – life of zanamivir) [72, 73]. It had exceptional *in vitro* activity against wild–type Influenza A and Influenza B viruses and also against most oseltamivir – resistant strains. Neuraminidase inhibitory activities of laninamivir *in vitro* against clinical isolates of influenza viruses were determined and these values were not changing significantly from year 2010 – 2013, suggesting that drug – resistant mutations don't emerge rapidly ($IC_{50} = 1.8 \times 10^{-9}$ M against strain A/California/07/2009) [74].

Because of the significant progress that has been done during development of zanamivir that led to the discovery of oseltamivir as a non – carbohydrate cyclohexene derivative, extensive effort has also been made in field of cyclopentane derivatives, resulting in the discovery of peramivir. Initially this inhibitor was designed to make multiple binding interactions with neuraminidase active site, allowing the antiviral to be effective against some viruses that were resistant to other anti – influenza drugs [75]. Peramivir was at first also developed as a oral agent, but it lacked sizeable antiviral effect because of low blood concentrations. Therefore it is now delivered intravenously and it is well suited for treating seriously ill patients that are not able to use inhaled or oral formulations [76]. Peramivir inhibitory activities against influenza viruses from clinical isolates *in vitro* provided lowest IC_{50} values among all for neuraminidase inhibitors in 2013 ($IC_{50} = 3.8 \times 10^{-10}$ M against

strain A/California/07/2009) and it had best inhibitory activity against Influenza B virus [74].

1.3.3 Tamiphosphor

One of the new neuraminidase inhibitors is tamiphosphor, oseltamivir derivative in which the carboxyl group from oseltamivir is replaced by a phosphonate group [77]. Phosphonate group is often used as bioisostere of carboxylate group in drug design. Tamiphosphor is shown in Figure 9.

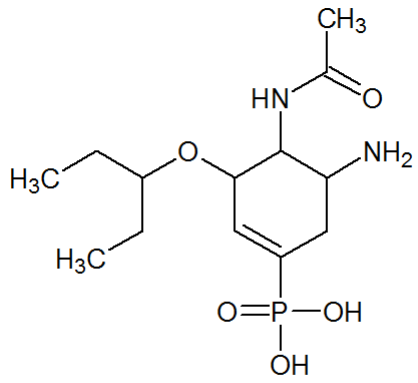

Figure 9: Tamiphosphor. Chemical formula was created by computer program ChemSketch.

Introduction of phosphonate group into oseltamivir structure showed to possess potent inhibitory activities against both human and avian influenza strain, including oseltamivir – resistant strain based on experiments with mice, cell culture assay and neuraminidase inhibition [78]. The phosphonate group is believed to make strong electrostatic interactions with guanidine moieties of three arginine residues (Arg 118, Arg 292 and Arg 371) because of the known oseltamivir orientation in neuraminidase active site and molecular docking experiments. Phosphonate ion in three dimensional structure is also topologically complementary to bind with the arginine residues in catalytic site. Inhibitory assay displayed similar results as laninamivir ($IC_{50} = 1.0 \times 10^{-9}$ M against strain A/WSN/1933) [79].

The urgency to develop novel anti – influenza drugs is not caused only by emergence of resistant viral strains as a antiviral treatment effect, but also because of antigenic drift that

constantly mutates viral proteins, especially surface glycoproteins, making neuraminidase a shifting target.

1.4 Influenza Resistance

The development of resistance has become an important concern, primarily in the case of Influenza A virus N1 subtypes which caused the latest pandemics and were the biggest threats among influenza strains in the first decade of 21st century [80]. The most attentively studied resistance is against oseltamivir, because of its wide use in influenza treatment. Influenza virus displays a high mutation rate, like other RNA viruses, due to the viral polymerase that is error – prone. Resistance against viral neuraminidase inhibitors can develop due to mutations in the neuraminidase active site and that can decrease the affinity towards the NA inhibitors [81].

1.4.1 Drug – resistant mutations

After treatment with influenza antivirotics, it is quite common that drug – resistant mutations occur and resulting mutated viral strain is not susceptible to subsequent therapy with the same inhibitor. In the case of adamantane inhibitors (M2 proton channel blockers) the resistance has been shown to develop rapidly, within 3 – 5 days in 30 – 50 % of treated patients (mutations V27A and S31N in M2 protein) [82]. Moreover, resistance against adamantane inhibitors has emerged so widely that H3N2 and H1N1 virus subtypes that cause majority of annual epidemics, are today intrinsically resistant to this class of inhibitors. Therefore the effectiveness of these compounds is very low and adamantane inhibitors are not recommended for treatment.

As a result of treatment with oseltamivir, the most common mutation that cause resistance are H274Y in group 1 neuraminidases and R292K in group 2 (described in N2 numbering) [83]. The H274Y mutation decreases sensitivity also to peramivir and the R292K mutation exhibits partial resistance to zanamivir. Both mutations in polypeptide chain are close to the active site of neuraminidase.

Influenza viruses with the H274Y mutation have been observed in patients treated with oseltamivir (and in some cases also with peramivir) as early as 48 hours after drugs were first administered [84]. According to several research studies, the H274Y – resistant virus

was detected also in many individuals that had no known anti – influenza drug exposure, which demonstrates the viable fitness and transmissibility of mutated virus. The inhibitory activity of oseltamivir against this mutation is significantly decreased (more than 750 – fold decrease in IC50 value; strain A/WSN/1933) [85].

The mechanism of resistance development with H274Y mutation consists in amino acid reposition in neuraminidase active site and the basis of complex formation. When influenza virus is treated, oseltamivir forms a hydrophobic interaction through 3 – pentyl side chain residue with hydrophobic pocket in active site, while sialic acid (as well as zanamivir) create hydrogen bond through the glycerol moiety from their side chain [86]. Within wild–type influenza virus both interactions are possible, but in the case of H274Y mutated neuraminidase, the introduced tyrosine's polar hydroxyl group repels the carboxyl group of glutamic acid at position 276, hydrophobic interaction through 3 – pentyl group of oseltamivir cannot be formed and treatment efficiency is dramatically decreased. Furthermore the mechanism of complex formation explains why neuraminidase with mutation H274Y is still able to bind sialic acid and hydrolyze glycosidic linkages and also why zanamivir is still a effective form of treatment, because creation of hydrogen bond between glycerol moiety and Glu276 is still possible. The difference in structure between wild–type and mutated neuraminidase (H274Y) interaction with oseltamivir is shown in Figure 10 on the next page.

Neuraminidase mutation R292K, as the most frequent mutation in group 2 subtype neuraminidases, acts in a similar fashion as mutation H274Y, positions numbers 274 and 292 are close to each other in active site [80]. If arginine at position 292 is changed by lysine, carboxyl group from glutamic acid at position 276 forms interactions with amino group from lysine, which changes the active site conformation and once again the hydrophobic stacking with 3 – pentyl side chain from oseltamivir is prevented. The inhibitory activity of oseltamivir is drastically decreased (over 10 000 – fold decrease in IC50 value; strain A/WSN/1933) and also inhibitory activity of zanamivir is reduced (over 130 – fold decrease in IC50 value; strain A/WSN/1933) [85]. The difference in structure and interaction with oseltamivir between wild–type and neuraminidase with mutation R292K is shown in Figure 11 on page 37.

Apart from two mutations H274Y and R292K, several other drug – resistant mutations occur in influenza virus strains, with lower incidence and not so dramatic decrease in

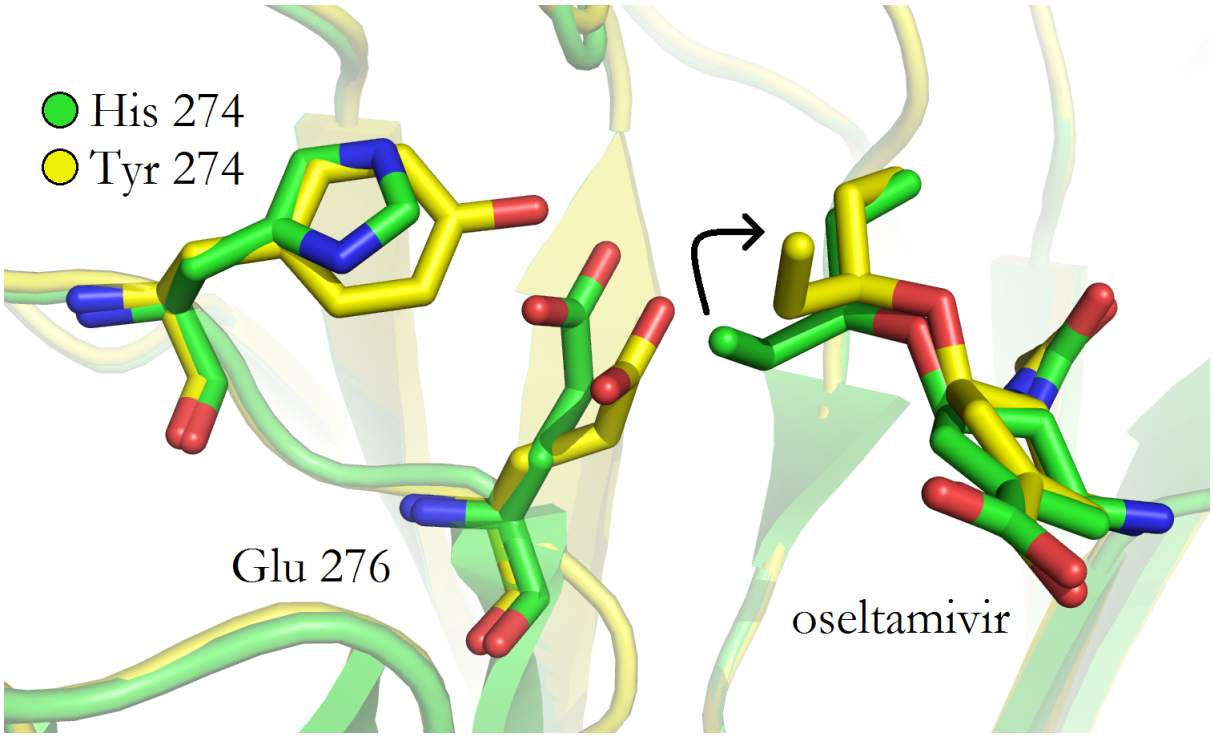

Figure 10: Structural alignment of wild–type and mutated (H274Y) neuraminidase active site with bound oseltamivir. wild–type neuraminidase with oseltamivir is depicted in green color; neuraminidase with mutation H274Y and corresponding oseltamivir is depicted in yellow color. Black arrow shows the shift of 3 – pentyl side chain from oseltamivir. More detailed description is provided in text. The image was created by computer program PyMOL from pdb files 2HU4 and 3CL0 [87, 88].

resistance [84]. Mutations at position 222, I222R and I222V, result in approximately 50 – fold decrease in IC50 value for oseltamivir (strain A/Sydney/5/1957 – like). Although this decrease is not as significant as previously described cases, mutations at position 222 combine together with H274Y mutation to form a double mutant with roughly 10 000 – fold decrease in IC50 value (strain A/Sydney/5/1957 – like), while the virus sustained its fitness and transmissibility. Other drug – resistant mutations include N294S, E116G, E116V, R371K, S246N [80].

1.4.2 Resistance statistics

Before the pandemics in 2009, the incidence of drug – resistant influenza viruses in patients treated with oseltamivir was 1 – 2 %. Between 2009 and 2012 the overall level of resistance against oseltamivir among H1N1 subtype strains has remained relatively low:

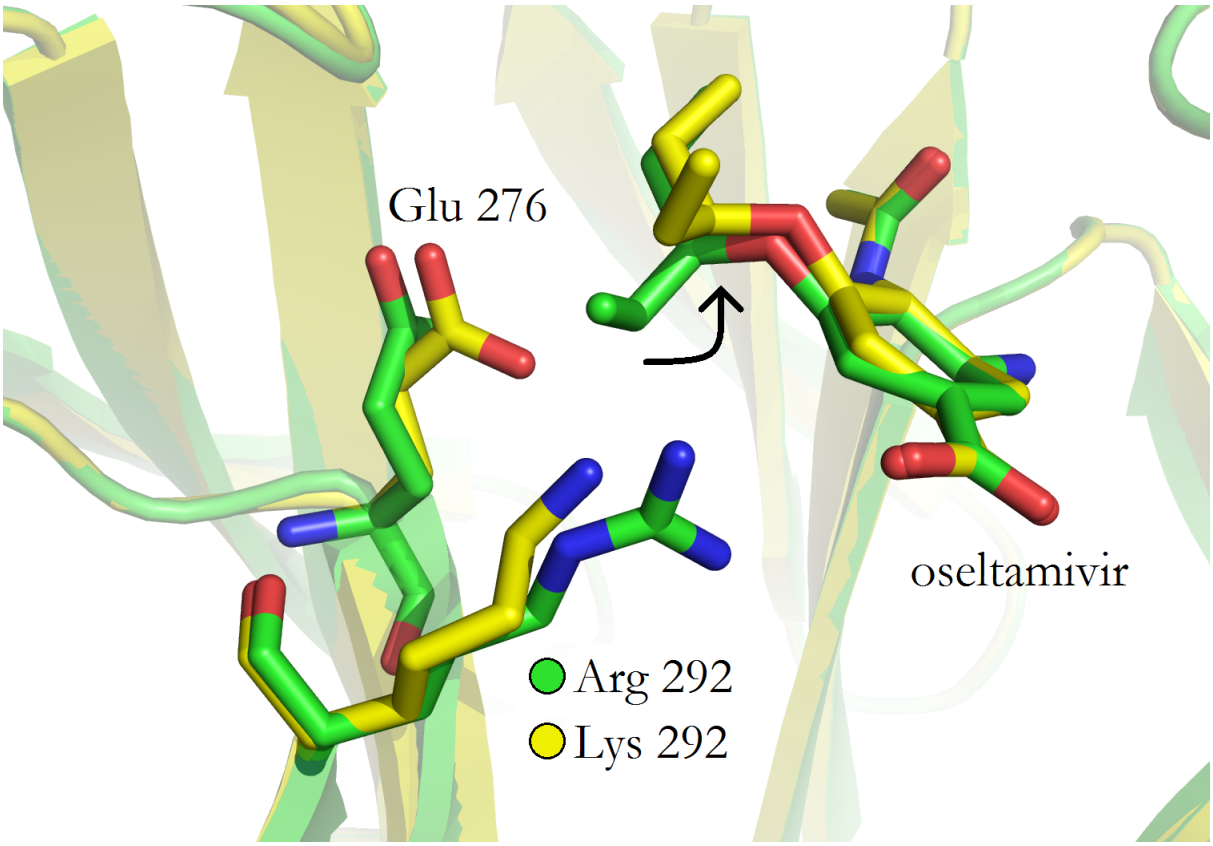

Figure 11: Structural alignment of wild–type and mutated (R292K) neuraminidase active site with bound oseltamivir. wild–type neuraminidase and oseltamivir is depicted in green color, neuraminidase with mutation R292K with oseltamivir is depicted in yellow color. More detailed description is provided in text. The image was created by computer program PyMOL from pdb files 4MWQ and 4MWW [89].

1 % in the United States, 2.5 % in Europe, less than 1 % in Canada and approximately 1.6 % worldwide [90]. However, drug – resistant influenza strains not associated with oseltamivir treatment has increased significantly in the USA, from 11 % in the 2009 – 2010 season to 74 % in 2010 – 2011, which confirm that oseltamivir – resistant viruses do not lose fitness and transmissibility.

The analysis of 15 studies in 2013 revealed 2.6 % influenza viruses (subtype H1N1) that were oseltamivir – resistant and no strains were resistant to zanamivir or peramivir [91]. Influenza strains resistant to oseltamivir have been predominantly observed in patients with prolonged viral replication during treatment with oseltamivir.

In 2014, the majority of circulating human influenza viruses (subtypes H1N1 and H2N3) were susceptible to all four neuraminidase inhibitors, while susceptibility towards

adamantane inhibitors is extremely low. Nevertheless the emergence of oseltamivir – resistant influenza variants highlight the need for epidemiological surveillance and vigilant monitoring [92, 93].

1.5 Influenza virus subtype H7N9

In early 2013, new human Influenza A virus strain subtype H7N9 emerged in China [94]. It was previously unknown avian influenza virus that had never infected humans and available data indicate that the virus originated by a two step reassortment process in birds.

1.5.1 H7 subtype viruses

In the first decade of 21st century, influenza infections with H7 viral subtype were observed. Numerous outbreaks of H7N7 and H7N3 influenza subtype infections were reported in the Netherlands and Canada with generally mild course of the disease, although also fatal cases occurred [95, 96]. The first three cases of human infection with H7N9 subtype influenza were observed in February 2013 in Shanghai municipality and Anhui province in China.

Whenever a new influenza virus strain outbreaks, the viral clinical isolates are investigated for already known molecular and genetic signatures [94]. In the first three cases with H7N9 subtype virus, the strains were designated as A/Anhui/1/2013, A/Shanghai/1/2013, and A/Shanghai/2/2013. Analysis proved that these strains have avian origin and emerged through two step reassortment with H9N2 subtype avian viral strain.

1.5.2 H7N9 infection

Every described human infection with novel H7N9 influenza virus was caused by direct contact with live poultry in markets or other avian species and no transmissibility from human to human has been observed [97]. Early symptoms of infection include fever, cough and overall weakness just like common flu. However the H7N9 virus causes extensive respiratory tract infection with breathing difficulties, progression to severe pneumonia and possible fatal outcome.

Because of the quite fast illness progression, early detection and quick antiviral treatment are essential for improving survival rates of H7N9 infection [98]. In the beginning of H7N9 epidemic in March 2013, investigation revealed a significant delay in diagnosis and treatment with antivirals, resulting in decreased efficiency of administered drugs. On the other hand, instant antiviral therapy with neuraminidase inhibitors improved patients' condition and possibly prevented higher mortality rate. In this case it is very important to follow the principle of early discovery, early reporting, early diagnosis and early treatment to further reduce the number of fatal cases.

1.5.3 Situation in years 2013 – 2014

Since the beginning of H7N9 epidemics in early 2013, the mortality rate of this influenza infection was exceptional. Out of the first three cases that were reported, two patients died. Until the end of March 2013, a total of 33 clinically confirmed human cases have been reported in Shanghai, while 18 patients died (almost 55 % mortality rate). After closures of poultry markets starting on 6th April 2013, reports of H7N9 human infections in Shanghai rapidly decreased, the virus was controlled in May and with exception of two cases in July, no new cases were detected in China until October 2013 [98, 99].

Nevertheless after the first wave of infection from March to May in 2013 which caused 44 deaths from 133 cases (approximately 33 % mortality rate), new cases of H7N9 infection were observed at the end of year 2013 with the start of winter season [100]. In the beginning of 2014 H7N9 broke out with even more cases than in 2013. Another 318 clinically approved cases were reported, out of which 121 people died [94]. Overall first and second wave of the infection brought 451 cases and 165 deaths (almost 37 % mortality rate) and H7N9 cases have been also discovered in Taiwan, Hong Kong and Malaysia. The progress of the first and the second wave is shown in Figure 12 on the next page.

Significant concerns have risen after discovery of H7N9 coinfection with H3N2 subtype [99]. The H3N2 subtype is common among seasonal influenza strains. It can easily infect people and most importantly it is transmissible from human to human. If a reassortment between these two viral subtypes occurred, a novel strain would potentially acquire the ability to transmit from person to person. In that case it is believed that such novel H7N9 would cause worldwide outbreak, because humans lack protective immune response to these types of viruses [102]. The situation is attentively monitored by World Health

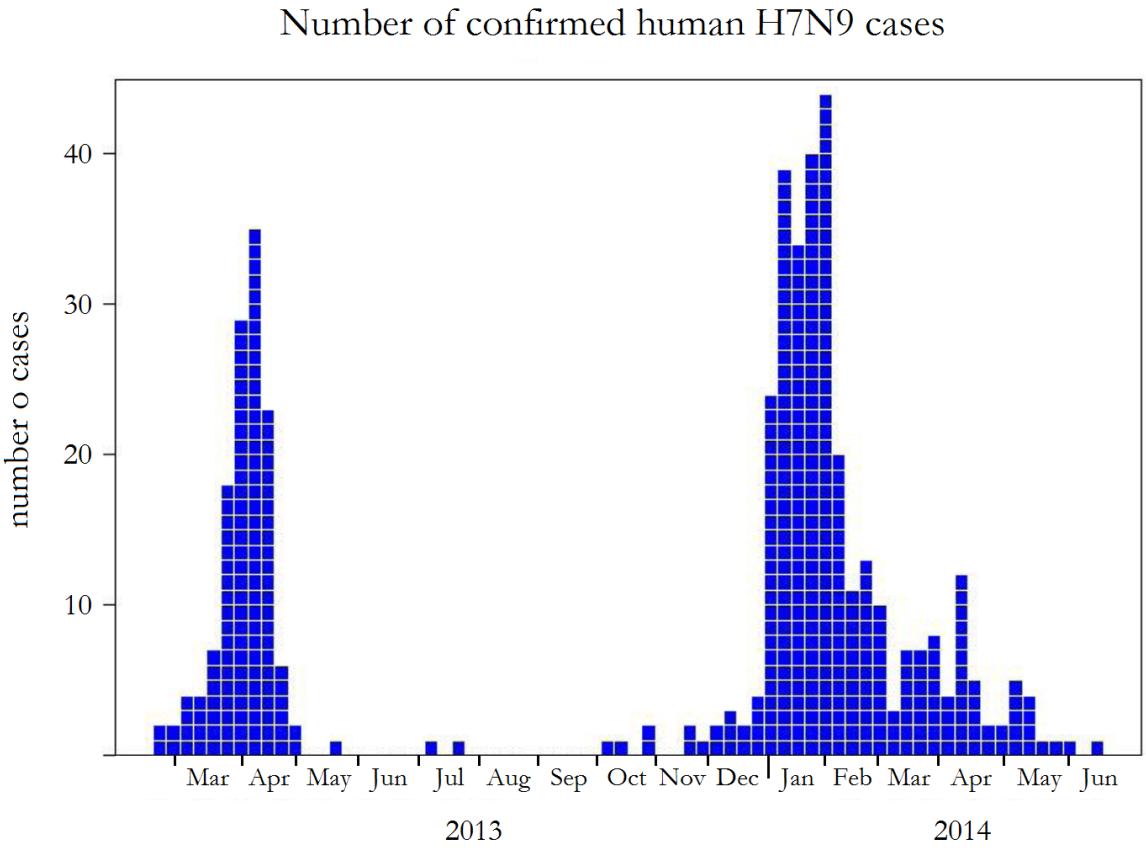

Figure 12: H7N9 infection from March 2013 to June 2014. Reproduced from [101].

Organization (WHO) and almost every new detected case is reported on WHO website.

1.5.4 H7N9 neuraminidase and treatment

Structurally and functionally, N9 neuraminidase from H7N9 strain A/Anhui/1/2013 is similar to other viral neuraminidases. On the other hand, identity with common neuraminidases that infect humans is roughly 45 % (compared with neuraminidase from pandemic H1N1 strain A/California/04/2009 and neuraminidase from seasonal H3N2 strain A/Texas/50/2012 which was used for vaccination before 2014 – 2015 flu season) [103]. Right from the first detection of novel virus, drug – resistance occurred, which is believed to be a result of treatment. In fact the first described strains, A/Anhui/1/2013 and A/Shanghai/1/2013, differ at only two positions of neuraminidase amino acid sequence. One polymorphism is located in the stalk region (position 40) and the other is one of three

conserved arginines located in active site (mutation R294K, which is equivalent to mutation R292K in N2 numbering that has been described in section 1.4.1 on page 34) [89]. Strain A/Shanghai/1/2013 is the resistant one, containing lysine at position 294. Mutation R294K causes extreme resistance against oseltamivir (over 100 000 – fold decrease in the affinity).

Despite R292K mutation has been previously described in naturally occurring viral neuraminidases, the corresponding N9 variant (R294K) has been observed only in strains isolated from patients that were treated with oseltamivir. Furthermore, influenza viruses with the R294K mutation exhibit compromised growth and fitness *in vitro*. After multiple cycles of replication, tested viruses reverted back to wild–type neuraminidase with arginine at position 294. Viruses with R294K mutation has been also found to be significantly less transmissible in ferret model system, suggesting that this position is crucial for N9 neuraminidase activity and limits transmissibility [104, 105, 106].

Novel H7N9 subtype influenza virus is also resistant to adamantane inhibitors and no vaccine for flu prevention is available, though several strain specific candidates have been developed [94]. Therefore, new research approaches to find efficient anti – influenza strategies are necessary to overcome influenza virus. Nevertheless viral neuraminidase is still the most promising drug target and best results among antivirotics were accomplished by targeting neuraminidase.

Winning the war against influenza viruses will probably either require combination therapy that would contain compounds against multiple viral proteins or development of highly successful universal vaccine that would eventually result in influenza eradication. Both strategies are far from this goal and intensive research is necessary in order to advance in general knowledge of influenza.

2 Diploma thesis aims

- Preparation, recombinant expression and purification of wild–type neuraminidase from influenza virus subtype H7N9 (strain A/Anhui/1/2013)
- Preparation, recombinant expression and purification of neuraminidase with mutation R294K from influenza virus subtype H7N9 (strain A/Shanghai/1/2013)
- Kinetic characterization of wild–type neuraminidase and mutant neuraminidase
- Thermodynamic characterization of complex formation of neuraminidase inhibitors oseltamivir carboxylate and tamiphosphor with wild–type neuraminidase and mutant neuraminidase
- Preparation of protein crystals for 3D structure determination by X–ray crystallography of wild–type neuraminidase with tamiphosphor

3 Materials and Methods

3.1 Materials and chemicals

- **Biotika**, Slovenská Ľupča (Slovak republic)
  Ampicillin
- **Fisher Scientific**, Hampton (USA)
  Decon 90
- **Gibco**, Waltham (USA)
  Sf – 900 II Serum – Free Media, 10 % fetal bovine serum, Defined Lipid Concentrate (100X), Yeastolate Ultrafiltrate (50X)
- **IBA**, Goettingen (Germany)
  BioLock Biotin blocking solution,
- **Lachema**, Brno (Czech Republic)
  bromphenol blue
- **Lach – Ner**, Neratovice (Czech Republic)
  ethanol, acetic acid, sodium acetate, hydrochloric acid, sodium chloride, sodium hydroxide, isopropanol, silver nitrate
- **New England BioLabs**, Ipswich (USA)
  BSA, restriction endonuclease *DpnI*
- **Penta**, Praha (Czech Republic)
  glycerol, methanol, formaldehyde
- **Promega**, Madison (USA)
  Phu DNA polymerase
- **SDT**, Baesweiler (Germany)
  casein buffer 20X – 4X concentrate
- **Serva**, Heidelberg (Germany)
  lysozyme
- **Sigma–Aldrich**, Bucks (Switzerland)
  SDS, DMSO, 2–mercaptoethanol, N, N‘–methylene bisacrylamide, TEMED, APS, sodium thiosulphate, sodium carbonate, disodium phosphate, monopotassium phosphate, potassium chloride, Monoclonal ANTI–FLAG M2–Peroxidase (HRP) antibody produced in mouse, ACES, Triton X–100, RNAse A, calcium chloride, HEPES,

desthiobiotin, HABA, MUNANA, 4–methylumbelliferone sodium salt, neuraminidase from *Clostridium perfingens*

- **Top–Bio**, Prague (Czech Republic)
  dNTP mix
- **USB**, Cleveland (USA)
  acrylamide, glycine, Tris, MES, Tween

3.2 Instruments

- centrifuges
  Biofuge – pico, Heraeus Instruments (Germany)
  Allegra X–15R, Beckman Coulter (USA)
  Avanti J–30I, Beckman Coulter (USA)
  Sorvall Evolution RC Centrifuge, Thermo Scientific (USA)
- rotary shaker Innova 44, Eppendorf (Germany)
- T–Gradient Thermocycler, Biometra (Germany)
- multimode reader Infinite M1000 PRO, Tecan (Switzerland)
- pH meter Unicam 9450, ATI Unicam (United Kingdom)
- vertical polyacrylamide gel electroforesis, Bio–Rad (USA)
- horizontal electrophoresis apparatus, Gibco (USA)
- Mini Trans – Blot Cell, Bio–Rad (USA)
- CCD camera ChemiDoc–It 600, UVP (United Kingdom)
- UV lamp UVT – 20 S/M/L, Herolab (Germany)
- spektrofotometer Specord 210, Chromspec (Czech Republic)
- incubator, Memmert (USA)
- sonicator Soniprep 150, Sanyo (USA)
- ThermoCell series MIXING BLOCK, BIOER (China)
- Nanodrop ND–1000 spectrophotometer, Thermo Scientific (USA)
- VP – ITC microcalorimeter, MicroCal – GE Healthcare Bio – Sciences (USA)

3.3 Bacterial strains, insects cells, plasmids and media

- Bacterial strain *Escherichia coli* TOP10, Invitrogen (USA)

- LB Broth, LB Agar, Sigma–Aldrich (Switzerland)
- plasmid pMT/BiP/V5–HisA, Invitrogen (USA)
- *Drosophila* Schneider S2 cells, Invitrogen (USA)

3.4 Other material

- dialysis membrane Spectrapor, Spectrum Laboratories (USA)
- Sterivex GP 0.22 μm Filter Unit, Millipore (USA)
- SuperSignal West Femto Maximum Sensitivity Substrate, Thermo Scientific (USA)
- QIAprep Spin Miniprep Kit, QIAGEN (USA)
- Plasmid Mega and Giga Kit, QIAGEN (USA)
- Centricon centrifugal filter devices, Millipore (USA)
- Strep – Tactin Sepharose 50 % suspension, IBA (Germany)
- Thrombin CleanCleav Kit, Sigma–Aldrich (Switzerland)
- BCA Protein Assay Kit, Thermo Scientific (USA)
- crystallization kits

  Crystallization Basic Kit for Proteins, Sigma–Aldrich (Switzerland)

  Crystallization Extension Kit for Proteins, Sigma–Aldrich (Switzerland)

  JCSG+ Suite, QIAGEN (USA)

All Blue Standard that was used as a marker for SDS – polyacrylamide gel electrophoresis is shown in Figure 13.

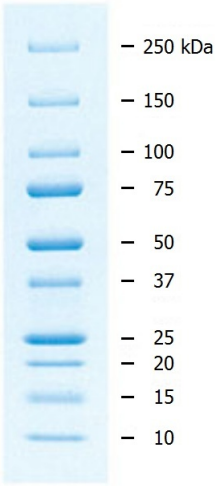

Figure 13: All Blue Standard. Reproduced from [107].

3.5 Neuraminidase gene

The gene for wild–type neuraminidase from viral strain A/Anhui/1/2013 (H7N9) in plasmid pMT/BiP/V5-HisA (Invitrogen), designated for expression in S2 insect cells, was purchased by Dr. Milan Kožíšek (IOCB). Apart from the neuraminidase gene, the construct in plasmid contained several tags and cleavage sites.

```
   1 ATGAAGTTAT GCATATTACT GGCCGTCGTG GCCTTTGTTG GCCTCTCGCT CGGGAGATCC
  61 TGGAGCCACC CCCAATTCGA GAAGGACTAC AAGGACGACG ACGACAAGGA GAACCTGTAC
 121 TTCCAGGGCA GATCCGCATG GAGCCACCCC CAATTCGAGA AGGGCTCTGA GAACCTGTAC
 181 TTCCAGGGCT CTGGCCTGCT TCCCCGTGCA TCCCGCAACT TCAACAATCT GACGAAGGGC
 241 CTGTGCACAA TCAACAGCTG GCACATTTAC GGAAAGGATA ATGCCGTGCG CATCGGAGAG
 301 AGCTCCGACG TGCTGGTGAC GCGCGAGCCA TACGTGTCCT GCGATCCAGA CGAGTGCCGC
 361 TTTTATGCCC TGAGCCAGGG CACAACCATC CGCGGAAAGC ACTCCAATGG CACCATTCAT
 421 GATCGCAGCC AGTACCGCGC CCTGATCTCC TGGCCACTGT CGAGTCCCCC GACGGTGTAT
 481 AACTCGCGCG TGGAGTGCAT TGGATGGAGC TCCACCAGTT GCCACGACGG CAAGAGCCGC
 541 ATGTCCATCT GCATTTCGGG CCCCAACAAT AACGCCTCCG CCGTGGTGTG GTACAATCGC
 601 CGCCCAGTGG CCGAGATCAA CACCTGGGCC CGCAATATTC TGCGCACGCA GGAGAGCGAG
 661 TGCGTGTGCC ATAACGGCGT GTGCCCAGTG GTGTTCACCG ATGGATCCGC CACGGGACCA
 721 GCCGACACAC GCATCTACTA TTTTAAGGAG GGAAAGATTC TGAAGTGGGA GAGCCTGACG
 781 GGCACAGCCA AGCACATCGA GGAGTGCTCC TGCTACGGAG AGCGCACCGG AATTACCTGC
 841 ACGTGCCGCG ATAACTGGCA GGGCAGCAAT CGCCCAGTGA TCCAGATTGA CCCCGTGGCC
 901 ATGACACATA CCTCGCAGTA CATCTGCAGT CCGGTGCTGA CGGATAATCC ACGCCCCAAC
 961 GACCCAAATA TTGGAAAGTG CAACGATCCG TACCCAGGCA ATAACAATAA CGGCGTGAAG
1021 GGATTCTCGT ATCTGGACGG AGCCAACACC TGGCTGGGAC GCACAATCAG TACCGCCTCG
1081 CGCAGTGGAT ACGAGATGCT GAAGGTGCCC AATGCCCTGA CAGATGACCG CTCCAAGCCG
1141 ATCCAGGGCC AGACCATTGT GCTGAACGCC GATTGGTCGG GCTACAGCGG ATCCTTCATG
1201 GATTATTGGG CCGAGGGAGA CTGCTACCGC GCCTGCTTTT ATGTGGAGCT GATCCGCGGA
1261 CGCCCAAAGG AGGACAAAGT GTGGTGGACC TCGAACAGTA TTGTGTCCAT GTGCAGCAGC
1321 ACGGAGTTTC TGGGACAGTG GAATTGGCCC GATGGAGCCA AGATTGAGTA TTTTCTG
```

Figure 14: DNA sequence of the neuraminidase construct (color highlights are explained in text).

```
  1 MKLCILLAVV AFVGLSLGRS WSHPQFEKDY KDDDDKENLY FQGRSAWSHP QFEKGSENLY
 61 FQGSGLVPRG SRNFNNLTKG LCTINSWHIY GKDNAVRIGE SSDVLVTREP YVSCDPDECR
121 FYALSQGTTI RGKHSNGTIH DRSQYRALIS WPLSSPPTVY NSRVECIGWS STSCHDGKSR
181 MSICISGPNN NASAVVWYNR RPVAEINTWA RNILRTQESE CVCHNGVCPV VFTDGSATGP
241 ADTRIYYFKE GKILKWESLT GTAKHIEECS CYGERTGITC TCRDNWQGSN RPVIQIDPVA
301 MTHTSQYICS PVLTDNPRPN DPNIGKCNDP YPGNNNNGVK GFSYLDGANT WLGRTISTAS
361 RSGYEMLKVP NALTDDRSKP IQGQTIVLNA DWSGYSGSFM DYWAEGDCYR ACFYVELIRG
421 RPKEDKVWWT SNSIVSMCSS TEFLGQWNWP DGAKIEYFL
```

Figure 15: protein sequence of the neuraminidase construct (color highlights are explained in text).

For both DNA and protein sequences (Figure 14 on the preceding page and Figure 15), in red is the BiP sequence, which is a signal sequence that leads the expressed protein out of the cells into media. The BiP sequence is cleaved by cells and the rest of protein is excreted into media. In magenta are two Strep–tags (Twin–Strep–tag), which bind to engineered streptavidin, called Strep – Tactin and proteins were purified via this interaction. In cyan color is FLAG–tag that was used for western blot development by ANTI–FLAG M2–Peroxidase antibody. In green, there are two cleavage sites, where proteins can be eventually cleaved by protease from Tobacco etch virus and in blue, there is thrombin cleavage site. For the purpose of this thesis, only thrombin cleavage site was used. Finally, the sequence in yellow is the head of neuraminidase N9 from strain A/Anhui/1/2013 that contains the catalytic segment of neuraminidase.

3.6 Site directed mutagenesis – polymerase chain reaction

- Pfu buffer: 20 mM Tris – HCl, pH 8.8; 10 mM $(NH_4)_2SO_4$; 10 mM KCl; 0.1 % (v/v) Triton X – 100; 0.1 mg/ml BSA

To obtain mutant neuraminidase from strain A/Shanghai/1/2013, which differs from wild–type neuraminidase by just one amino acid (R294K), polymerase chain reaction was performed. The primers were designed so the final product would carry point mutation R294K. Primer sequences (underlined triplets code lysine instead of arginine):

1. primer: 5' – CC TGC ACG TGC AAG GAT AAC TGG CAG – 3'

2. primer: 5' – CTG CCA GTT ATC CTT GCA CGT GCA GG – 3'

The polymerase chain reaction was performed in Pfu buffer. The template DNA was the construct of wild–type neuraminidase N9 in plasmid pMT/BiP/V5–HisA (described in section 3.5 on page 46). The composition of the reaction (total volume 45 μl) is shown in Table 1.

Table 1: The composition of the polymerase chain reaction for site directed mutagenesis.

template DNA	$\sim$ 10 μg/ml
1. primer	0.5 μM
2. primer	0.5 μM
dNTP mix	0.25 mM
Phu DNA polymerase	0.5 U

The site directed mutagenesis – polymerase chain reaction was performed by T–Gradient Thermocycler (Biometra). The conditions of the reaction are in Table 2.

Table 2: Polymerase chain reaction conditions – individual cycles and temperature setting.

1 cycle	95°C	30 s
16 cycles	95°C	30 s
	55°C	1 min
	68°C	5 min
1 cycle	72°C	8 min
cooling	4°C	

After polymerase chain reaction was completed, 1 μl of restriction endonuclease *DpnI* (New England BioLabs) was added to the mixture to cut the template DNA at 37°C overnight. Next day, this final PCR mixture was used for transformation of bacterial cells.

3.7 Transformation of competent bacterial cells

Suspension of competent bacterial cells *E. coli* TOP10 (70 μl) was gently mixed with 10 μl of the final PCR mixture with plasmid pMT/BiP/V5–HisA containing gene for mutated neuraminidase (R294K). The suspension was left for 5 minutes on ice, subsequently the plasmid DNA was transformed into the bacterial cells by a heat shock performed at 42°C for 90 seconds, which was followed by 5 minutes incubation on ice. Then, 0.8 ml of sterile LB Broth was added to the cells and the suspension was incubated at 37°C for 1 hour, before spreading the mixture on agar plates containing Ampicillin (100 μg/ml). The agar plates coated with the transformed cells were incubated at 37°C overnight.

3.8 Minipreparation of plasmid DNA

- buffer I: 50 mM Tris – HCl, pH 8.0; 10 mM EDTA; 0.25 mg/ml RNase A; 1.4 mg/ml lysozyme
- buffer II: 200 mM NaOH; 1 % (w/v) SDS
- buffer III: 3 M potassium acetate, pH 5.5
- acetate buffer: 3 M sodium acetate, pH 5.2
- buffer QG: 20 mM Tris – HCl, pH 6.6; 5.5 M guanidine thiocyanate
- buffer PE: 10 mM Tris – HCl, pH 7.5; 80 % (v/v) ethanol

Several authentic colonies that have grown after transformation of competent cells were separately transferred into 15 ml of LB Broth and shaken 220 RPM at 37°C overnight. The cell cultures were then centrifuged (4000g, 6 min, 4°C), supernatants were wasted, 245 μl of buffer I were added to cell pellets in microtubes and suspensions were left for 5 minutes on ice. Then, 450 μl of buffer II were added to each microtube and suspensions were left for 10 minutes on ice. Next, 338 μl of buffer III were added to microtubes, the mixtures were vortexed, left for another 10 minutes on ice and then centrifuged (15000g, 6 min, 20°C). Supernatants were transferred to new tubes, 30 μl of acetate buffer, 338 μl of isopropanol and 200 μl of buffer QG were added.

After vortexing, the solutions were applied on QIAprep spin columns from QIAprep Spin Miniprep Kit (QIAGEN), then centrifuged (15000g, 1 min) and flow – through solution was discarded. Then, 700 μl of buffer PE were added on columns and after centrifugation (15000g, 1 min) flow – through solution was wasted. Finally 45 μl of sterile

distilled water were applied on columns and flow – through solution contained prepared DNA.

To determine concentration and purity of prepared DNA, measurements on Nanodrop spectrophotometer (Thermo Scientific) were performed. To check, whether prepared DNA has correct sequence, the final samples were sequenced at GATC Biotech (Germany) and one colony of originally transformed *E. coli* TOP10 cells with correct sequence was selected for maxipreparation of DNA.

3.9 Maxipreparation of plasmid DNA

- buffer P1: 50 mM Tris – HCl, pH 8.0; 10 mM EDTA; 10 μg/ml RNase A
- buffer P2: 200 mM NaOH, 1 % (w/v) SDS
- buffer P3: 3 M potassium acetate, pH 5.5
- buffer QBT: 50 mM MOPS, pH 7.0; 750 mM NaCl; 15 % (v/v) isopropanol; 0.15 % (v/v) Triton X – 100
- buffer QC: 50 mM MOPS, pH 7.0; 1 M NaCl; 15 % (v/v) isopropanol
- buffer QF: 50 mM Tris – HCl, pH 8.5; 1.25 M NaCl; 15 % (v/v) isopropanol
- buffer TE: 10 mM Tris – HCl, pH 8.0; 1 mM EDTA

For maxipreparation of plasmid DNA using Plasmid Mega and Giga Kit (QIAGEN), 500 ml of sterile LB Broth with Ampicillin (100 μg/ml) were inoculated with 1 colony of competent *E. coli* TOP10 cells that were previously transformed with DNA plasmid pMT/BiP/V5–HisA with neuraminidase gene. Bacterial culture was incubated in rotary shaker Innova (Eppendorf) at 37°C and 220 RPM overnight.

After incubation, the bacterial culture was centrifuged (6000g, 4°C, 15 min), supernatant was removed and cell pellet was resuspended in 50 ml of buffer P1, then 50 ml of buffer P2 were added, the mixture was stirred and incubated for 5 minutes at room temperature. Then, 50 ml of cold buffer P3 were added and after stirring, the mixture was left for 30 minutes on ice. The suspension was then centrifuged (25000g, 30 min, 4°C). Equilibration of QIAGEN – tip 2500 from the kit with 35 ml of buffer QBT followed. After centrifugation, the supernatant was filtrated through gauze and applied to the QIAGEN – tip. The tip was washed with 200 ml of buffer QC and then the DNA was eluted with 35 ml of buffer QF. The purified DNA was precipitated by 24.5 ml of isopropanol, the

mixture was centrifuged (15000g, 30 min, 4°C), supernatant was removed and pellet was washed by 7 ml of 70 % ethanol. The suspension was centrifuged (15000g, 10 min, 4°C), supernatant was removed and the pellet was air dried for 20 minutes. Finally the pellet was dissolved in 400 μl of buffer TE and concentration and purity of prepared DNA were measured by Nanodrop spectrophotometer (Thermo Scientific).

3.10 Stable transfection of S2 cells using calcium phosphate

- solution A: 0.24 M $CaCl_2$; 9 μg of plasmid DNA (coding wild–type or mutated neuraminidase) from maxipreparation; 0.5 μg of pCoBLAST
- solution B: 50 mM HEPES, pH 7.14; 1.5 mM Na_2HPO_4; 280 mM NaCl

For transfection, *Drosophila* Schneider S2 cells (Invitrogen) were cultured in 35 mm plate in Sf – 900 II Serum – Free Media (Gibco), supplemented with 10 % fetal bovine serum (Gibco) at 25°C until they reached density of $2 - 4 \times 10^6$ cells/ml. Solution A (300 μl) was added dropwise to 300 μl of solution B while vortexing and the final mixture was incubated for 40 minutes at room temperature. Solution A contained selective plasmid pCoBLAST, which provided cells with resistance against blasticidin – S. Next, the solution was mixed, added dropwise to the cells and the cells were incubated for 16 – 24 hours at 25°C.

The transfected cells were then transferred to 15 ml sterile falcon tube and centrifuged (500g, 2 min). The medium was decanted, 3 ml of fresh Sf – 900 II Serum – Free Media with 10 % fetal bovine serum (complete media) were added, the cells were replaced into a new plate and incubated for 24 hours at 25°C. The media was then carefully aspirated and 3 ml of fresh complete media containing blasticidin – S (final concentration 5 μg/ml) were added. This selective media was replaced every 4 – 5 days, until resistant cells started growing (approximately 3 weeks).

3.11 Expression of recombinant viral neuraminidase

Stably transfected Schneider S2 cells resistant to blasticidin – S of concentration minimally 1×10^7 cells/ml were transferred into 100 ml of Sf – 900 II Serum – Free Media to final concentration approximately 1×10^6 cells/ml and this mixture was transferred into sterile 250 ml spinner flask for expression. Then, 1 ml of Defined Lipid Concentrate

(Gibco) and 2 ml of Yeastolate Ultrafiltrate (Gibco) were added into the mixture. Cell culture was incubated at 25°C and stirred at 100 RPM, until the density reached 1×10^7 cells/ml (2 – 4 days).

Then, the cell culture was transferred into bigger flask (3000 ml), another 400 ml of Sf – 900 II Serum – Free Media were added together with 4 ml of Defined Lipid Concentrate and 8 ml of Yeastolate Ultrafiltrate and cell culture was incubated again (25°C, 100 RPM). After the density reached 1×10^7 cells/ml, expression of recombinant viral neuraminidase was induced by addition of 100 mM $CuSO_4$ (to final concentration 1 mM). On the first and third day after induction, the media was supplemented with 2.5 ml of 200 mM L – glutamine and 5 ml of 20 % D – glucose in sterile water. The cell density and the recombinant protein production was checked on daily basis and cell culture was harvested once protein production wasn't increasing. The mixture was then centrifuged ($500g$, 30 min, 25°C), decanted media containing recombinant protein was centrifuged again ($3360g$, 30 min, 4°C) and subsequently stored at – 80°C before further processing.

3.12 Protein purification

- wash buffer: 100 mM Tris – HCl, pH 8.0; 150 mM NaCl
- elution buffer: 100 mM Tris – HCl, pH 8.0; 150 mM NaCl; 10 mM desthiobiotin
- regeneration buffer: 100 mM Tris – HCl, pH 8.0; 150 mM NaCl; 1 mM HABA

For protein purification, approximately 500 ml of media were processed. First, 1.2 ml of BioLock solution (IBA) were added to media, which is solution of avidin. It binds biotin in medium that would interfere with Strep–tags binding to Strep – Tactin (IBA). The media was then filtered through Sterivex GP 0.22 μm Filter Unit (Millipore) The purification was performed on 1 ml of Strep – Tactin Sepharose resin in plastic column (IBA) that selectively bind Strep–tagged proteins. The flow of solution through the column was mediated only by gravity.

To equilibrate the column, 4 ml of wash buffer were added. After equilibration, the media containing expressed proteins was gradually applied on column and flow – through fraction was collected. Next, 10 ml of wash buffer were applied to the column and wash fraction wash gathered. Then, 4 ml of elution buffer were added and first elution fraction was collected. Another 4 ml of elution buffer were applied to obtain second elution

fraction, finally 4 ml of elution buffer were added and third elution fraction was collected. After elution was complete, the column was regenerated by addition of approximately 20 ml of regeneration buffer, which changed color of column to red and then wash buffer ($\sim$ 20 ml) was applied until the resin was colorless again. The whole process of purification was monitored with SDS – polyacrylamide gel electrophoresis and western blot, protein concentrations were determined and enzyme activity of individual fractions was measured.

3.13 Proteolytic cleavage of protein tag

- buffer T: 50 mM Tris – HCl, pH 8.0; 150 mM NaCl; 10 mM $CaCl_2$
- buffer TW: 50 mM Tris – HCl, pH 8.0; 10 mM $CaCl_2$
- buffer TR1: 50 mM Tris – HCl, pH 8.0
- buffer TR2: 50 mM Tris – HCl, pH 8.0; 500 mM NaCl
- buffer TRG: 20 mM Tris – HCl, pH 8.0; 50 % (v/v) glycerol

After purification of recombinant protein was complete, proteolytic cleavage of protein tag followed to obtain only the head of viral neuraminidase. Several elution fractions with purified recombinant protein were merged ($\sim$ 60 ml) and dialysed against buffer T at 4°C overnight in dialysis membrane (Spectrapore) of molecular weight cut off 6 – 8 kDa.

The solution of recombinant protein was then transferred to plastic tube and 0.5 ml of thrombin – agarose conjugate in buffer TW from Thrombin CleanCleav Kit (Sigma–Aldrich) were added and the mixture was left on tube roller at laboratory temperature overnight. The sample was then centrifuged (500g, 6 min, 20°C), supernatant was carefully aspirated and thrombin – agarose conjugate from pellet was regenerated after final protein fraction was acquired.

The protein solution was applied on equilibrated Strep – Tactin Sepharose resin in plastic column (IBA) (see section 3.12 on the previous page for information about buffers and column) and the flow – through solution contained final fraction of purified viral neuraminidase head. After the flow – through was collected, 4 ml of elution buffer were applied on column, elution fraction was collected and the column was regenerated. The proteolytic cleavage of protein tag was monitored with SDS – polyacrylamide gel electrophoresis and western blot, protein concentrations were determined and enzyme activity of selected fractions was measured.

The regeneration of thrombin – agarose conjugate (per 250 μl of conjugate mixture):

1. added 0.5 ml of buffer TR2; centrifuged (500g, 2 min, 20°C); supernatant wasted
2. added 0.5 ml of buffer TR1; centrifuged (500g, 2 min, 20°C); supernatant wasted
3. added 0.5 ml of buffer TR2; centrifuged (500g, 2 min, 20°C); supernatant wasted
4. added 0.5 ml of buffer TR1; centrifuged (500g, 2 min, 20°C); supernatant wasted
5. again added 0.5 ml of buffer TR1; centrifuged (500g, 2 min, 20°C); supernatant wasted
6. added 0.5 ml of buffer TRG and sample was stored at 4°C

3.14 Protein concentration determination

To determine protein concentration, BCA Protein Assay Kit (Thermo Scientific) was used. First, 25 μl of protein solutions were pipetted into 96 well plate, together with 25 μl of BSA solutions of known concentrations (0.0125 mg/ml; 0.025 mg/ml; 0.05 mg/ml; 0.1 mg/ml; 0.2 mg/ml). Then, working reagent was prepared by mixing 50 parts of BCA Reagent A with 1 part of BCA Reagent B (200 μl of BCA Reagent A was required per protein sample). Next, 200 μl of working reagent was added to each protein solution in 96 well plate and the plate was incubated for 30 minutes at 37°C. After incubation, absorbance at 562 nm was measured on multimode reader Infinite M1000 PRO (Tecan) and protein concentration were determined by calibration curve of BSA solutions of known concentrations.

3.15 Enzyme activity determination and kinetic characterization

- buffer MES: 100 mM MES, pH 6.15; 150 mM NaCl; 10 mM $CaCl_2$

Enzyme activity was determined by substrate for fluorometric assay of neuraminidase called MUNANA (2'–(4–methylumbelliferyl)–D–N–acetylneuraminic acid). For the purpose of control, whether individual fractions contain active enzyme and purification analysis, 2 μl of protein solution were added to buffer MES containing 250 μM substrate MUNANA (total volume 40 μl). The mixture was incubated for 1 hour (37°C, 900 RPM) on mixing block (BIOER). After incubation, the reaction was stopped by addition of 40 μl of 1 M Na_2CO_3, individual samples were transferred into 96 well plate and fluorescence emission at 450 nm was measured after excitation at 365 nm on multimode reader Infinite

M1000 PRO (Tecan).

For the purpose of kinetic characterization, 3 μl of protein solution (concentration of protein 2.9 μM) were added to buffer MES solutions containing several different substrate concentrations (5 μM – 3000 μM, total reaction volume 40 μl). The same incubation, stopping of the reaction and subsequent measurement as in the previous case followed. To determine k_{cat} value, emission at 450 nm after excitation at 365 nm was measured also for 4–methylumbelliferone (sodium salt), the product of the reaction.

The MUNANA substrate was also used to detect activity of several different neuraminidases during overnight cleavage. The experiment was performed in 80 μl of buffer MES containing 500 μM substrate MUNANA. The activity was detected for 100 nM wild–type neuraminidase N9 (from viral strain A/Anhui/1/2013), 100 nM mutated R294K neuraminidase N9 (from viral strain A/Shanghai/1/2013), 100 nM wild–type neuraminidase N1 (from viral strain A/California/07/2009) and 60 nM neuraminidase from *Clostridium perfingens*. Recombinant viral neuraminidases were prepared in the laboratory of doc. Jan Konvalinka in insects cells (for more information see section 3.10 on page 51) and neuraminidase from *Clostridium perfingens* was purchased from Sigma–Aldrich. For control purposes, enzyme free measurements were performed for substrate MUNANA and product 4–methylumbelliferone. All samples were incubated at 37°C overnight and then analysed by HPLC – MS measurements (Ing. Radko Souček, IOCB).

3.16 SDS – polyacrylamide gel electrophoresis

- sample buffer (6x): 350 mM Tris – HCl, pH 6.8; 30 % (v/v) glycerol; 350 mM SDS; 4 % (v/v) 2 mM 2 – mercaptoethanol; 180 μM bromphenol blue
- electrode buffer (5x): 140 mM Tris – HCl, pH 8.8; 1.4 M glycine; 20 mM SDS

Expression, purification and cleavage of protein tag was monitored by SDS – polyacrylamide gel electrophoresis. Stacking gel (6.6 %) and resolving gel (16 %) for each analysis was prepared from a stock solution of 44 % (w/v) acrylamide (42.8 % acrylamide and 1.2 % N, N‘ – methylene bisacrylamide) as follows:

- 16 % gel: 375 mM Tris – HCl, pH 8.8; 16 % acrylamide; 0.1 % (w/v) SDS; 0.1 % (v/v) TEMED; 0.1 % (w/v) APS

- 6.6 % gel: 375 mM Tris – HCl, pH 6.8; 6.6 % acrylamide; 0.1 % (w/v) SDS; 0.2 % (v/v) TEMED; 0.1 % (w/v) APS

The samples were denatured by boiling for 5 minutes with the sample buffer. The electrophoresis was performed in a vertical electrophoresis apparatus (Bio–Rad) for 90 minutes in a constant voltage of 140 V. For visualization of separated proteins, the gels were stained by silver:

1. fixing (30 min): 12 % (v/v) acetic acid; 50 % (v/v) methanol; 0.02 % (v/v) formaldehyde
2. washing (3 × 15 min): 50 % (v/v) methanol
3. reduction (1 min): 0.02 % (w/v) sodium thiosulphate
4. washing (3 × 20 s): distilled water
5. impregnation (20 min): 0.2 % (w/v) silver nitrate; 0.02 % (v/v) formaldehyde
6. washing (3 × 20 s): distilled water
7. development (10 s – 5 min): 566 mM sodium carbonate, 16 μM sodium thiosulphate, 0.02 % (v/v) formaldehyde
8. washing (3 × 20 s): distilled water
9. stopping (10 min): 12 % (v/v) acetic acid; 50 % (v/v) methanol

3.17 Western blotting with chemiluminescent detection

- transfer buffer: 192 mM glycine; 25 mM Tris – HCl; 10 % (v/v) methanol
- buffer PBS: 10 mM Na_2HPO_4; 1.8 mM KH_2PO_4, pH 7.4; 137 mM NaCl; 2.7 mM KCl; 0.05 % Tween

After SDS – polyacrylamide gel electrophoresis, the gel was equilibrated with nitrocellulose membrane in transfer buffer for 5 minutes. Proteins in gel were then electroblotted to the membrane in Mini Trans – Blot Cell (Bio–Rad) at constant voltage 100 V for 60 minutes. Then, the membrane was blocked in 10 ml of casein buffer (SDT) for 60 minutes at laboratory temperature and subsequently the membrane was incubated with 5 μl of ANTI–FLAG M2–Peroxidase antibody (Sigma–Aldrich, final concentration $\sim$5 μg/ml) overnight at 4°C.

The membrane was rinsed in buffer PBS, then developed by SuperSignal West Femto Maximum Sensitivity Substrate (Thermo Scientific), dried and placed in transparent plas-

tic foil. The chemoluminescence signal was detected using CCD camera ChemiDoc–It 600 (UVP).

3.18 Protein crystallization

- crystallization buffer: 5 mM Tris – HCl, pH 8.0

Purified neuraminidase head from strain A/Anhui/1/2013 was concentrated up to 9 mg/ml using centricon centrifugal filter (Millipore). During this process, the protein solution was concentrated, buffer was exchanged to crystallization buffer and inhibitor tamiphosphor was added to final 3–molar excess.

For crystallization trials, 0.5 ml of crystallization solutions (from crystallization kits) was pipetted into 15 well plate with removable covers. On the inside of individual covers, 1 μl of protein solution was mixed with 1 μl of crystallization solution and the mixture was left as hanging drop for protein crystallization. The cover was fastened, the plate was left at 18°C and checked regularly.

3.19 Isothermal titration calorimetry

- buffer NA – ITC: 50 mM MES, pH 6.15; 150 mM NaCl; 10 mM $CaCl_2$
- buffer NA – ITC 2: 50 mM ACES, pH 6.15; 150 mM NaCl; 10 mM $CaCl_2$

The solution of purified protein was dialysed against buffer NA – ITC at 4°C overnight in dialysis membrane (Spectrapore) of molecular weight cut off 6 – 8 kDa. After dialysis, the solution of protein was concentrated using centricon centrifugal filter (Millipore) of molecular weight cut off 10 kDa up to concentration required for ITC titration. The concentration of neuraminidase inhibitor solution was 12.5 × higher that concentration of protein in calorimetric cell. Exact concentrations were determined by HPLC amino acid analysis (Radko Souček, IOCB) for protein and by elemental analysis (Stanislava Matějková, IOCB) for inhibitors. The protein solution and NA – ITC buffer itself were degassed by stirring under vacuum before measurement.

Before titration experiment, the cell and syringe of microcalorimeter was treated by detergent and cleaned with distilled water. Calorimetric measurements were performed in VP – ITC microcalorimeter (MicroCal – GE Healthcare Bio – Sciences). Titration started with 2 μl injection of neuraminidase inhibitor solution, followed by 30 injections of

9 μl of neuraminidase inhibitor solution that were added to the protein solution in cell in 300 seconds intervals. The experiment was kept at 25°C. After titration, inhibitor's heat of dilution was determined by repeating the experiment, this time with buffer NA – ITC itself (protein free) in the cell. The whole experiment was repeated in buffer NA – ITC 2 for determination of potential protonation effects during titration. Measurements were analysed by software that was developed by MicroCal, Inc. in computer program Origin.

4 Results

Two variants of neuraminidase head domain from influenza H7N9 subtype strains A/Anhui/1/2013 and A/Shanghai/1/2013 were expressed in *Drosophila* Schneider S2 cells and then purified in sufficient amount and purity for kinetic characterization, isothermal titration calorimetry and protein crystallography. Exemplary purification of wild–type neuraminidase (A/Anhui/1/2013) is demonstrated in sections 4.2 and 4.3. The overall results of all purifications with yields and purity analysed by SDS – polyacrylamide gel electrophoresis are described in section 4.4. The kinetic characterization, ITC experiments and protein crystallization results are described in sections 4.5 – 4.8.

4.1 DNA manipulation

The plasmid coding mutated viral neuraminidase (from strain A/Shanghai/1/2013) was prepared using site directed mutagenesis – polymerase chain reaction. Mutation R294K was created using specifically designed primers and DNA template that encoded wild–type neuraminidase. The product of mutagenesis was transformed to competent bacterial cells and several colonies were chosen for minipreparation of plasmid DNA. After minipreparation was successfully performed and the sequencing was done, plasmid DNA of correct sequence was prepared in higher amount by maxipreparation. Concentration of DNA, absorbance ratio of 260 nm to 280 nm and also absorbance ratio of 260 nm to 230 nm was determined by Nanodrop ND−1000 spectrophotometer after maxipreparation ($c_{DNA} = 862\,\mu g/ml$; $A_{260/280} = 1.91$; $A_{260/230} = 2.19$).

4.2 Protein purification

wild–type viral neuraminidase N9 and its mutated variant R294K were produced in *Drosophila* Schneider S2 cells. Expression of recombinant proteins was induced by addition of $CuSO_4$ to final concentration 1 mM. Insect cells produced well soluble recombinant proteins that were secreted into media. Viral neuraminidase was purified from 500 ml of media using Strep – Tactin Sepharose resin (IBA). The expression and purification of recombinant proteins was monitored by SDS – polyacrylamide gel electrophoresis and western blot (Figure 16 on the next page).

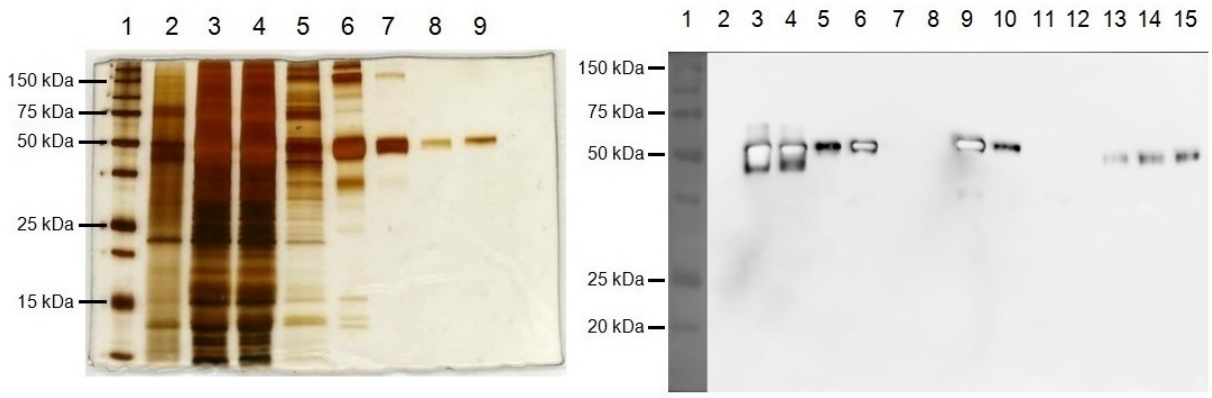

Figure 16: SDS – polyacrylamide gel electrophoresis (left) and western blot (right) of purification samples. **SDS – PAGE**: lane 1, 0.8 μl of All Blue Standard; lane 2, 10 μl of media without expression; lane 3, 10 μl of media with N9 neuraminidase expression; lane 4, 10 μl of flow – through fraction after Strep – Tactin resin; lane 5, 10 μl of washing fraction of Strep – Tactin resin; lane 6, 4 μl of first elution fraction; lane 7, 4 μl of second elution fraction; lane 8, 4 μl of third elution fraction; lane 9, 6 μl of NA standard N9 (0.1 μg). **Western blot**: lane 1, 2 μl of All Blue Standard; lane 2, 1 μl of media without expression; lane 3, 1 μl of media with N9 neuraminidase expression; lane 4, 1 μl of flow – through fraction after Strep – Tactin resin; lane 5, 1 μl of washing fraction of Strep – Tactin resin; lane 6, 1 μl of first elution fraction (20 $\times$ diluted); lane 7, 1 μl of second elution fraction (20 $\times$ d.); lane 8, 1 μl of third elution fraction (20 $\times$ d.); lane 9, 2 μl of first elution fraction (10 $\times$ d.); lane 10, 2 μl of second elution fraction (10 $\times$ d.); lane 11, 2 μl of third elution fraction (10 $\times$ d.); lane 12, 2.5 μl of NA standard N1 (2.5 ng); lane 13, 5 μl of NA standard N1 (5 ng); lane 14, 7.5 μl of NA standard N1 (7.5 ng); lane 15, 10 μl of NA standard N1 (10 ng).

The purification was also analysed by enzyme assay and protein concentrations were determined in order to obtain purification table (Table 3).

Table 3: Purification table monitoring the progress of wild–type neuraminidase N9 purification. V – volume; c_p – protein concentration; a – activity; a_s – specific activity, P_c – purification coefficient

fraction	V [ml]	c_p [mg/ml]	a [RFU $\times 10^{-5}$]	a_s [RFU $\times 10^{-5}$/mg]	P_c
media with N9	500	2.39	11055.3	9.3	1.0
flow – through f.	500	2.50	6646.3	5.3	0.6
washing f.	40	0.46	306.9	16.7	1.8
1. elution f.	16	0.40	3012.6	481.1	51.9
2. elution f.	16	0.07	343.8	330.8	35.7
3. elution f.	16	0.02	0.0	0.0	0.0

4.3 Proteolytic cleavage of protein tag

Selected elution fractions that contained active and pure neuraminidase, were merged for thrombin cleavage of protein tag. The cleavage procedure was monitored by SDS – polyacrylamide gel electrophoresis and western blot (Figure 17). The flow – through fraction (line 4 of SDS – polyacrylamide gel electrophoresis) was the final sample that was used for further experiments.

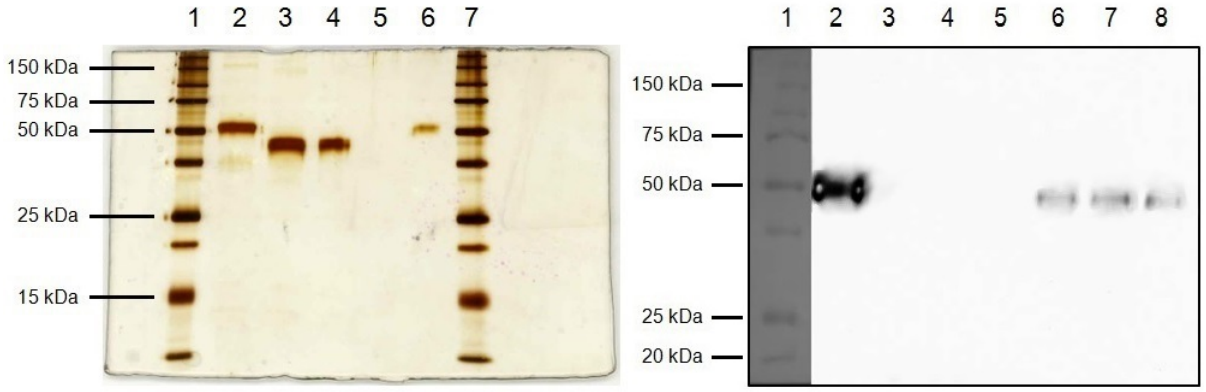

Figure 17: SDS – polyacrylamide gel electrophoresis (left) and western blot (right) of proteolytic cleavage procedure. **SDS – PAGE**: lane 1, 0.8 μl of All Blue Standard; lane 2, 2.5 μl of sample before cleavage by thrombin; lane 3, 2.5 μl of sample after cleavage by thrombin; lane 4, 2.5 μl of flow – through fraction after Strep – Tactin resin; lane 5, 2.5 μl of elution fraction; lane 6, 6 μl of NA standard N9 with protein tag (0.1 μg); lane 7, 0.8 μl of All Blue Standard. **Western blot**: lane 1, 2 μl of All Blue Standard; lane 2, 0.5 μl of sample before cleavage by thrombin; lane 3, 0.5 μl of sample after cleavage by thrombin; lane 4, 0.5 μl of flow – through fraction after Strep – Tactin resin; lane 5, 0.5 μl of elution fraction; lane 6, 1 μl of NA standard N1 (5 ng); lane 7, 1.5 μl of NA standard N1 (7.5 ng); lane 8, 2 μl of NA standard N1 (10 ng).

4.4 Purification results

Wild–type neuraminidase N9 was successfully purified, as well as its variant with mutation R294K. Overall purification results were monitored by SDS – polyacrylamide gel electrophoresis (Figure 18 on the following page), Table 4 on the next page summarizes purification yields for both recombinant proteins.

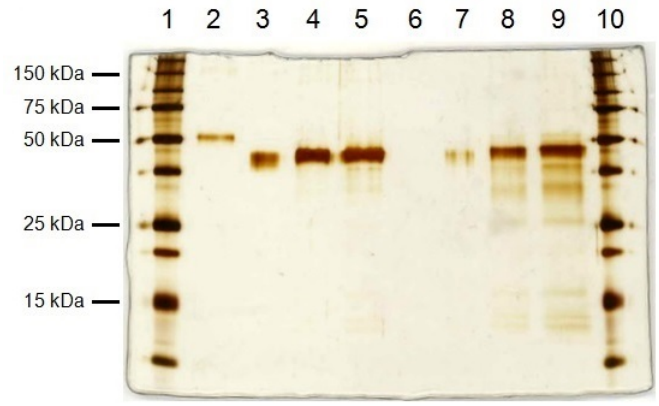

Figure 18: SDS – polyacrylamide gel electrophoresis of final recombinant protein samples. lane 1, 0.8 μl of All Blue Standard; lane 2, 6 μl of NA standard N9 with protein tag (0.1 μg); lane 3, 0.75 μl of wild–type N9 (0.1 μg); lane 4, 3.7 μl of wild–type N9 (0.5 μg); lane 5, 7.5 μl of wild–type N9 (1 μg); lane 7, 1.3 μl of mutant R294K N9 (0.1 μg); lane 8, 6.5 μl of mutant R294K N9 (0.5 μg); lane 9, 13 μl of mutant R294K N9 (1 μg); lane 10, 0.8 μl of All Blue Standard.

Table 4: Total yields of purified recombinant proteins after expression in insect cells.

protein	yield from 500 ml of media
wild–type neuraminidase N9 (A/Anhui/1/2013)	15.6 mg
R294K neuraminidase N9 (A/Shanghai/1/2013)	5.3 mg

4.5 Detection of enzyme activity of prepared neuraminidases

The overnight cleavage of MUNANA substrate by several neuraminidases is shown in Figure 19 on the following page. Three different viral neuraminidases were used for experiment (wild–type neuraminidase N1 from pandemic 2009 strain, wild–type neuraminidase N9 from 2013 strain and its variant neuraminidase N9 with mutation R294K). For control measurement, also neuraminidase from *Clostridium perfingens* was used. Wild–type neuraminidase N9 cleaved 16 % of MUNANA substrate during overnight cleavage. Activity of neuraminidase N9 with mutation R294K could not be detected, because it did not cleave the substrate at all. Wild–type neuraminidase N1 cleaved almost 80 % of substrate and neuraminidase from *Clostridium perfingens* processed 100 % of the substrate. Experiment details are in section 3.15 on page 54.

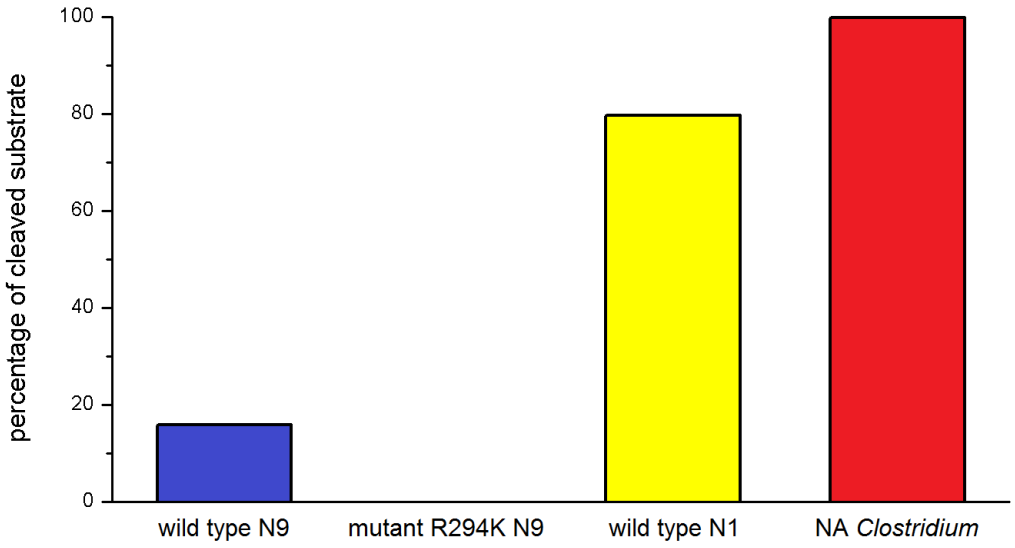

Figure 19: Enzyme activity detection. Percentage of cleaved substrate MUNANA (500 μM) by three viral neuraminidases (wild–type N9, mutant R294K N9, wild–type N1) and neuraminidase from *Clostridium perfingens*. The measurement was performed in buffer 100 mM MES, pH 6.15; 150 mM NaCl; 10 mM $CaCl_2$

4.6 Kinetic characterization

Wild–type neuraminidase N9 from viral strain A/Anhui/1/2013 was kinetically characterized using MUNANA substrate of different concentrations and 240 nM neuraminidase. The K_{m} value was 1100 μM, the k_{cat} value was 0.015 s^{-1} and the ratio k_{cat}/K_m was 14 $M^{-1}s^{-1}$. The kinetic characterization is shown in Figure 20 on the following page, kinetic parameters derived from characterization are in Table 5. The data set was analysed by computer program GraFit.

Table 5: Kinetic parameters for wild–type neuraminidase N9 derived from kinetic characterization.

parameter	value
k_{cat}	$0.015 \pm 0.001\ s^{-1}$
K_m	$1100 \pm 180\ \mu M$
k_{cat}/K_m	$14 \pm 1\ M^{-1}s^{-1}$

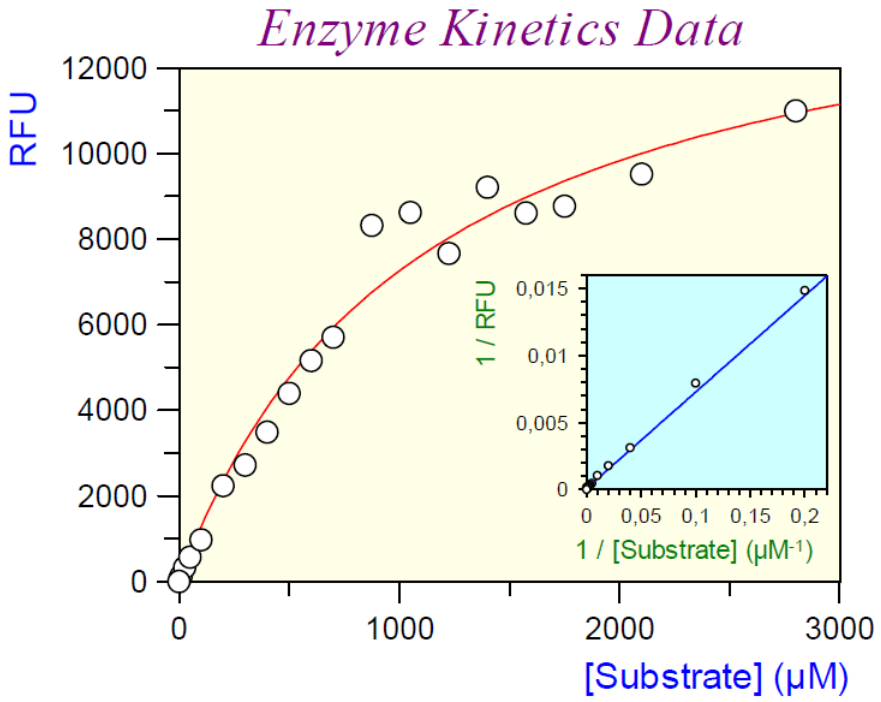

Figure 20: Kinetic characterization of wild–type neuraminidase N9. The smaller graph represents the Lineweaver – Burk plot. Measurement was performed with various concentrations of MUNANA substrate in buffer 100 mM MES, pH 6.15; 150 mM NaCl; 10 mM $CaCl_2$

4.7 Thermodynamic analysis

Viral neuraminidase forms a complex with inhibitor oseltamivir carboxylate, which prevents the release of virus progeny on the surface of infected cells. Tamiphosphor is a oseltamivir derivative that contains phosphonate group. This novel inhibitor performed well against various influenza strains, including oseltamivir – resistant strain. Complex formation of both inhibitors with wild–type neuraminidase N9 was thermodynamically analysed by VP – ITC microcalorimeter (MicroCal).

During titration experiments, a small amount of inhibitor was titrated into the microcalorimeter cell, containing wild–type neuraminidase. Upon binding, exothermic pulses were observed. These pulses were integrated, adjusted by control experiment and final titration curves are shown in Figures 21 and 22 on the following page.

The thermodynamic analysis was performed in two buffers (MES and ACES) for determination of potential protonation effects during titration. Interaction of oseltamivir carboxylate with wild–type neuraminidase N9 was accompanied by favorable enthalpy

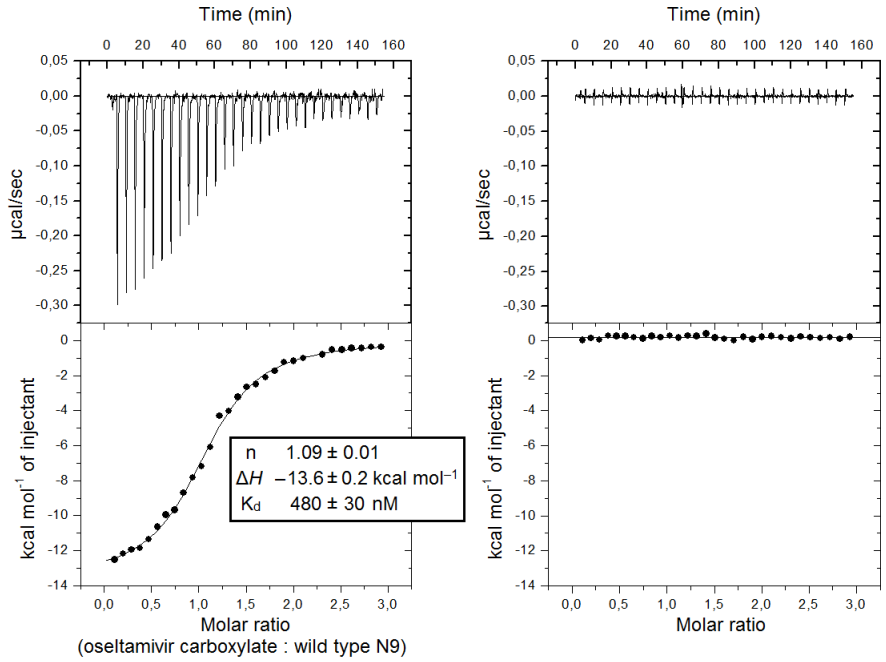

Figure 21: Isothermal titration calorimetry of wild–type neuraminidase N9 with oseltamivir carboxylate (in MES buffer). The graph on right shows control titration (enzyme free).

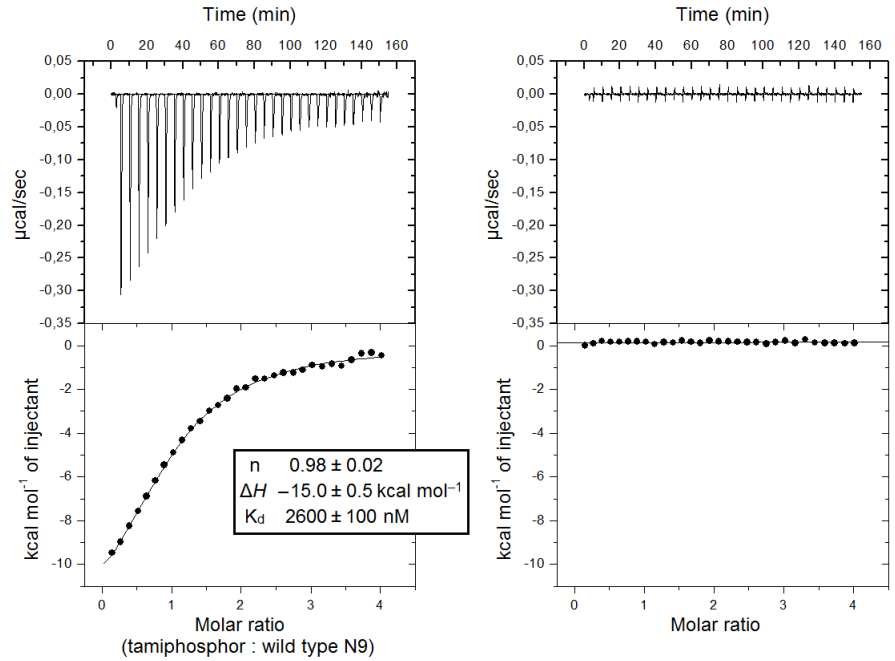

Figure 22: Isothermal titration calorimetry of wild–type neuraminidase N9 with tamiphosphor (in MES buffer). The graph on right shows control titration (enzyme free).

change ($-13.6\,kcal \cdot mol^{-1}$) and unfavorable entropy change ($-T\Delta S = 4.8\,kcal \cdot mol^{-1}$). Stoichiometry was determined as 1.14 and dissociation constant value was 390 nM. In the case of tamiphosphor, the complex formation with wild–type neuraminidase N9 was also accompanied by favorable enthalpy change ($-14.6\,kcal \cdot mol^{-1}$) and unfavorable entropy change ($-T\Delta S = 6.9\,kcal \cdot mol^{-1}$). Stoichiometry of interaction was 1.04 and value of dissociation constant was 2100 nM. The overall results are shown in Figure 23 and Table 6.

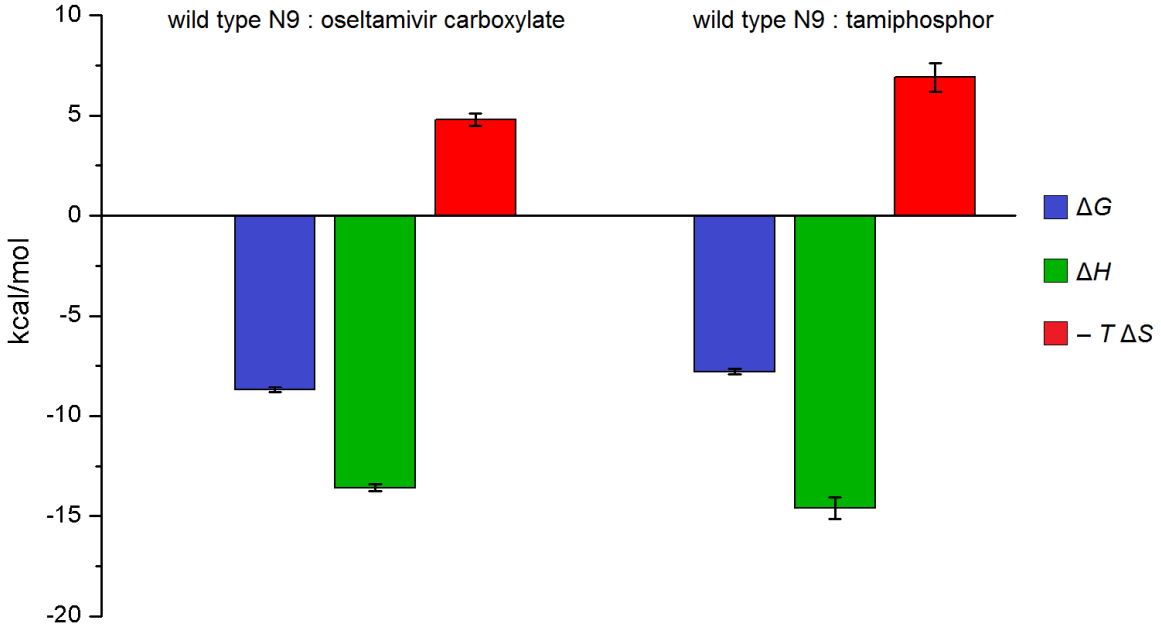

Figure 23: Individual contributions of Gibbs free energy change, enthalpy change and entropy change to binding of oseltamivir carboxylate and tamiphosphor to wild–type neuraminidase N9.

Table 6: Thermodynamic parameters results for binding of oseltamivir carboxylate and tamiphosphor to wild–type neuraminidase N9.

	oseltamivir carboxylate : N9	tamiphosphor : N9
stoichiometry	1.14 ± 0.05	1.04 ± 0.06
$K_d \quad (nM)$	390 ± 80	2100 ± 460
$\Delta G \quad (kcal \cdot mol^{-1})$	– 8.7 ± 0.1	– 7.8 ± 0.1
$\Delta H \quad (kcal \cdot mol^{-1})$	– 13.6 ± 0.2	– 14.6 ± 0.5
$-T\Delta S \quad (kcal \cdot mol^{-1})$	4.8 ± 0.3	6.9 ± 0.7

4.8 Protein crystallization

Cocrystallization trials of wild–type neuraminidase N9 with tamiphosphor were performed in solutions from crystallization kits (Crystallization Basic Kit for Proteins, Crystallization Extension Kit for Proteins; Sigma–Aldrich and JCSG+ Suite; QIAGEN). Viral neuraminidase did not create monocrystals suitable for X–ray crystallography in any solutions. Most of the droplets either contained precipitates or they were clear even 6 months after the trials began. Results of two cocrystallization trials are shown in Figure 24.

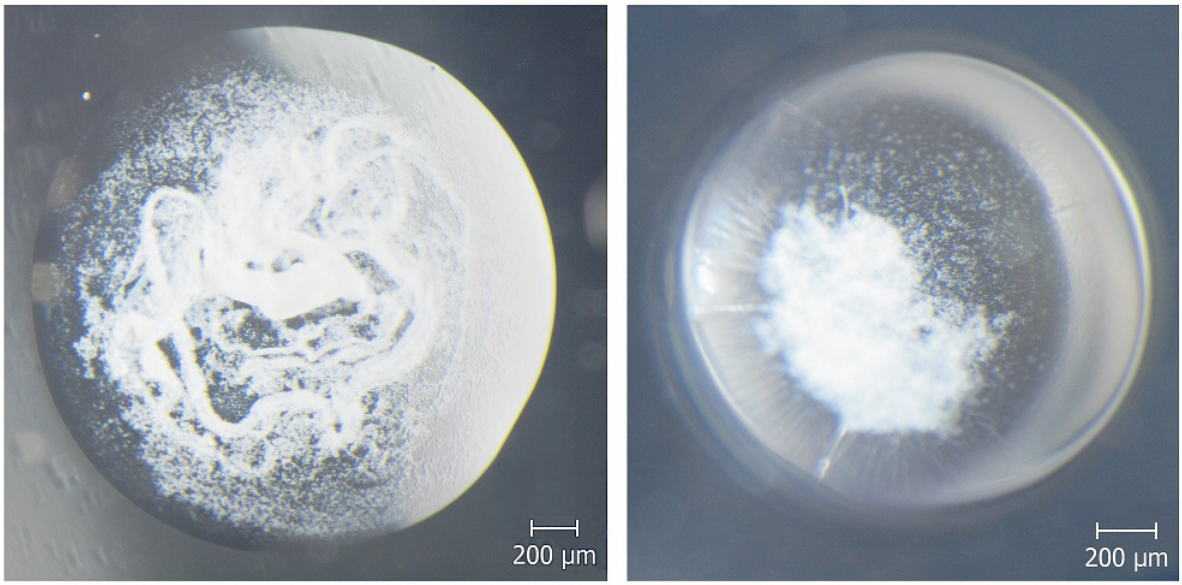

Figure 24: Results of two cocrystallization trials. Only precipitates can be seen in both droplets.

5 Discussion

Influenza virus causes a widespread infectious disease with outbreaks occurring especially during winter season. Although the course of the disease can be unpleasant, in most cases patients fully recover. However, even seasonal influenza can be deadly, primarily among very young and old people. In addition, new influenza strains emerge after a reassortment of different viral strains and these novel strains are very dangerous due to no preexisting immunity in humans. Development of new and successful anti – influenza strategies is therefore upon highest importance.

One of the possible treatment approaches is targeting viral proteins that are necessary for viral life cycle, with inhibitors that would prevent virus from spreading. Among individual proteins, viral neuraminidase appears to be very promising target. It is an enzyme present on the surface of virions and plays crucial role in viral progeny release from infected cells. For the purpose of this thesis, experiments were performed with head domain of neuraminidase N9 from influenza strain A/Anhui/1/2013.

Since viral neuraminidase requires posttranslational modification for proper function, it was essential to use relatively complicated eukaryotic expression system for expression and purification instead of simpler prokaryotic one (e.g. *Escherichia coli*). Neuraminidase coding sequence was first ligated into plasmid pMT/BiP/V5–HisA that allows heterologous expression in *Drosophila* Schneider S2 cells. The whole expressed protein contained Twin–Strep–tag for affinity purification and FLAG–tag for western blotting development.

Section 4.2 on page 59 describes the purification of expressed recombinant protein. Results of SDS – polyacrylamide gel electrophoresis and western blot in Figure 16 on page 60 show that pure protein was obtained after single purification step and that flow – through fraction still contained purified protein. Recombinant wild–type neuraminidase was therefore purified from flow – through fraction until the FLAG–tagged protein couldn't be detected on western blot (total of 9 purification cycles). Overall, the purification was successful, with decent yields of both recombinant proteins (15 mg of wild–type neuraminidase and 5 mg of mutant neuraminidase from 500 ml of media).

After recombinant neuraminidases were purified, detection of enzyme activity followed (Figure 19 on page 63). In the case of wild–type neuraminidase N9, enzyme activity could be detected, although only 16 % of substrate was cleaved compared to 100 % of

cleaved substrate by neuraminidase from *Clostridium perfingens* (no traces of substrate were observed). On the other hand, activity of mutant R294K neuraminidase N9 couldn't be detected at all, when result of overnight cleavage was almost identical to the control, enzyme free reaction. The enzyme activity of neuraminidase N1 from pandemic strain A/California/07/2009 was also detected as a control and it happened to be much more active than N9 neuraminidase, when it cleaved almost 80 % of substrate. Because no activity of mutant R294K neuraminidase N9 could be observed, it wasn't used for further experiments.

Results of kinetic characterization of wild–type neuraminidase N9 show reason for low enzyme activity (Table 5 on page 63). The k_{cat}/K_m value was only 14 $M^{-1}s^{-1}$, and so the efficiency of substrate processing was much lower than in case of neuraminidase N1 from last pandemic 2009 strain, which had much higher processivity and k_{cat}/K_m value of 818 $M^{-1}s^{-1}$ (measured in laboratory of doc. Jan Konvalinka; data not shown in results section).

The thermodynamic analysis of complex formation of viral neuraminidase with approved inhibitor has never been published. Within this thesis, the first thermodynamic characterization of complex formation of wild–type N9 neuraminidase with oseltamivir carboxylate as well as its derivative tamiphosphor was performed.

Thermodynamic analysis of neuraminidase inhibitor interactions with wild–type neuraminidase N9 shows that both characterized inhibitors (oseltamivir carboxylate and tamiphosphor) successfully bind to neuraminidase. During ITC experiments, these thermodynamic parameters were determined – stoichiometry of interaction, dissociation constant of the complex, enthalpy and entropy changes. Stoichiometry of interaction was for both inhibitors determined as 1:1 to neuraminidase monomer. Dissociation constant values revealed that oseltamivir carboxylate forms approximately five times stronger binding complex with wild–type neuraminidase N9 (390 nM) than tamiphosphor (2100 nM).

Complex formation of neuraminidase and oseltamivir carboxylate is driven by favorable enthalpy change ($-13.6\,kcal \cdot mol^{-1}$). Creation of hydrogen bonds and other electrostatic interactions contribute the most to the enthalpy change, thus in this case, the complex formation is driven by creation of strong direct interactions between inhibitor and enzyme. On the other hand, the the entropic contribution to binding of oseltamivir carboxylate is unfavorable ($-T\Delta S = 4.8\,kcal \cdot mol^{-1}$). Entropy change is more complicated to interpret,

but favorable contribution is usually caused by release of solvent from interacting molecules and unfavorable contribution is caused by reduction of degrees of freedom for individual molecules. Binding of oseltamivir carboxylate is presumably accompanied by restrictions of molecule variability that contributes negatively to the interaction.

In the case of tamiphosphor, complex formation with neuraminidase is also driven by enthalpy change, in even more favorable fashion than during oseltamivir carboxylate binding (for tamiphosphor $\Delta H = -14.6 kcal \cdot mol^{-1}$). So, the substitution of carboxyl group in oseltamivir carboxylate structure by phosphonate group very likely create stronger electrostatic interactions with three arginine residues (in N2 numbering Arg 118, Arg 292, Arg 371) in neuraminidase active site (described in section 1.3.3 on page 33). Nevertheless the complex formation is accompanied by even more unfavorable entropy change ($-T\Delta S = 6.9\, kcal \cdot mol^{-1}$), than in the case of oseltamivir carboxylate, which results in overall weaker interaction. The negative contribution in entropy change might be caused by burial of hydrophilic phosphonate group that could be restricted in the binding pocket of neuraminidase.

Thermodynamic measurements were performed in two different buffers in order to determine potential protonation effects during titration. For both oseltamivir carboxylate and tamiphosphor, no protonation was observed during complex formation.

The best binding inhibitors are those with both enthalpy and entropy favorable contributions. Oseltamivir carboxylate is a first generation inhibitor that can be chosen as a starting point for development of novel inhibitors with better thermodynamic properties of complex formation.

Tamiphosphor was chosen for cocrystallization trials, because there was no three – dimensional structure of neuraminidase N9 with this inhibitor. Nevertheless these trials were not successful, even though over one hundred of different crystallization solutions were used. Most of the droplets contained precipitates of various appearance and in order to obtain monocrystals of sufficient quality for X–ray crystallography, cocrystallization trials need to be optimized.

6 Conclusions

Wild–type neuraminidase N9 from influenza strain A/Anhui/1/2013 was expressed in insect expression system and then successfully purified. Yield of the purification was sufficient for further experiments. With the same procedure, neuraminidase N9 with mutation R294K (from strain A/Shanghai/1/2013) was successfully expressed and purified as well.

Kinetic parameters for wild–type neuraminidase N9 were determined, on the other hand no enzyme activity was detected for mutant R294K neuraminidase.

The first thermodynamic analyses ever of complex formation of wild–type neuraminidase N9 with two inhibitors (oseltamivir carboxylate and tamiphosphor) were performed. The measurements revealed that both inhibitors successfully bind neuraminidase and in both cases the interaction is driven by favorable enthalpy change.

Cocrystallization trials of wild–type neuraminidase N9 with tamiphosphor were not successful and protein crystals were not obtained. Crystallization conditions need to be optimized.

References

[1] *WHO | Influenza (Seasonal).* `http://www.who.int/mediacentre/factsheets/fs211/en/`; cited: December 27th 2014.

[2] Johnson, N. P. A. S.; Mueller, J. Updating the accounts: global mortality of the 1918-1920 "Spanish" influenza pandemic. *Bulletin of the History of Medicine.* **2002**, *76*, 105–115.

[3] Nelson, M. I.; Holmes, E. C. The evolution of epidemic influenza. *Nature Reviews Genetics.* **2007**, *8*, 196–205.

[4] Fouchier, R. A. M.; Munster, V.; Wallensten, A.; Bestebroer, T. M.; Herfst, S.; Smith, D.; Rimmelzwaan, G. F.; Olsen, B.; Osterhaus, A. D. M. E. Characterization of a novel influenza A virus hemagglutinin subtype (H16) obtained from black-headed gulls. *Journal of Virology.* **2005**, *79*, 2814–2822.

[5] Hay, A. J.; Gregory, V.; Douglas, A. R.; Lin, Y. P. The evolution of human influenza viruses. *Philosophical Transactions of the Royal Society B: Biological Sciences.* **2001**, *356*, 1861–1870.

[6] Fauquet, C. M.; Fargette, D. International Committee on Taxonomy of Viruses and the 3,142 unassigned species. *Virology Journal.* **2005**, *2*, 64.

[7] Suzuki, Y. Sialobiology of influenza: molecular mechanism of host range variation of influenza viruses. *Biological and Pharmaceutical Bulletin.* **2005**, *28*, 399–408.

[8] Lu, L.; Lycett, S. J.; Brown, A. J. L. Reassortment patterns of avian influenza virus internal segments among different subtypes. *BMC evolutionary biology.* **2014**, *14*, 16.

[9] Tong, S.; Zhu, X.; Li, Y.; Shi, M.; Zhang, J.; Bourgeois, M.; Yang, H.; Chen, X.; Recuenco, S.; Gomez, J. New world bats harbor diverse influenza A viruses. *PLoS pathogens.* **2013**, *9*, e1003657.

[10] Burke, D. F.; Smith, D. J. A Recommended Numbering Scheme for Influenza A HA Subtypes. *PloS one.* **2014**, *9*, e112302.

[11] Lynch, J. P.; Walsh, E. E. Influenza: evolving strategies in treatment and prevention. *Seminars in Respiratory and Critical Care Medicine*. **2007**, *28*, 144–158.

[12] Yen, H.-L.; Webster, R. G. Pandemic influenza as a current threat. *Current Topics in Microbiology and Immunology*. **2009**, *333*, 3–24.

[13] Rajagopal, S.; Treanor, J. Pandemic (avian) influenza. *Seminars in Respiratory and Critical Care Medicine*. **2007**, *28*, 159–170.

[14] Martin, P. M. V.; Martin-Granel, E. 2,500-year evolution of the term epidemic. *Emerging Infectious Diseases*. **2006**, *12*, 976–980.

[15] Smith, F. B. The Russian Influenza in the United Kingdom, 1889–1894. *Social History of Medicine*. **1995**, *8*, 55–73.

[16] Trilla, A.; Trilla, G.; Daer, C. The 1918 "Spanish flu" in Spain. *Clinical Infectious Diseases: An Official Publication of the Infectious Diseases Society of America*. **2008**, *47*, 668–673.

[17] Taubenberger, J. K.; Reid, A. H.; Janczewski, T. A.; Fanning, T. G. Integrating historical, clinical and molecular genetic data in order to explain the origin and virulence of the 1918 Spanish influenza virus. *Philosophical Transactions of the Royal Society B: Biological Sciences*. **2001**, *356*, 1829–1839.

[18] Taubenberger, J. K.; Morens, D. M. 1918 Influenza: the mother of all pandemics. *Emerging Infectious Diseases*. **2006**, *12*, 15–22.

[19] Knobler, S.; Mack, A.; Mahmoud, A.; Lemon, S. The Threat of Pandemic Influenza: Are We Ready? Workshop Summary. *The National Academies Press*. **2005**, 60–61.

[20] Laver, G.; Garman, E. Pandemic influenza: its origin and control. *Microbes and infection*. **2002**, *4*, 1309–1316.

[21] Potter, C. W. A history of influenza. *Journal of applied microbiology*. **2001**, *91*, 572–579.

[22] Wertheim, J. O. The Re-Emergence of H1N1 Influenza Virus in 1977: A Cautionary Tale for Estimating Divergence Times Using Biologically Unrealistic Sampling Dates. *PLoS ONE*. **2010**, *5*, e11184.

[23] Zimmer, S. M.; Burke, D. S. Historical perspective–Emergence of influenza A (H1N1) viruses. *The New England Journal of Medicine*. **2009**, *361*, 279–285.

[24] Pfister, R.; Kochanek, M.; Leygeber, T.; Brun-Buisson, C.; Cuquemelle, E.; Machado, M. B.; Piacentini, E.; Hammond, N. E.; Ingram, P. R.; Michels, G. Procalcitonin for diagnosis of bacterial pneumonia in critically ill patients during 2009 H1N1 influenza pandemic: a prospective cohort study, systematic review and individual patient data meta-analysis. *Critical Care (London, England)*. **2014**, *18*, R44.

[25] Trifonov, V.; Khiabanian, H.; Rabadan, R. Geographic dependence, surveillance, and origins of the 2009 influenza A (H1N1) virus. *The New England Journal of Medicine*. **2009**, *361*, 115–119.

[26] Ferguson, N. M.; Cummings, D. A. T.; Fraser, C.; Cajka, J. C.; Cooley, P. C.; Burke, D. S. Strategies for mitigating an influenza pandemic. *Nature*. **2006**, *442*, 448–452.

[27] Meng, Z.; Han, R.; Hu, Y.; Yuan, Z.; Jiang, S.; Zhang, X.; Xu, J. Possible pandemic threat from new reassortment of influenza A(H7N9) virus in China. *Euro Surveillance: Bulletin Européen Sur Les Maladies Transmissibles = European Communicable Disease Bulletin*. **2014**, *19*.

[28] Bouvier, N. M.; Palese, P. The biology of influenza viruses. *Vaccine*. **2008**, *26 Suppl 4*, D49–53.

[29] Harrison, S. C. Viral membrane fusion. *Nature Structural & Molecular Biology*. **2008**, *15*, 690–698.

[30] Stevens, J.; Blixt, O.; Tumpey, T. M.; Taubenberger, J. K.; Paulson, J. C.; Wilson, I. A. Structure and receptor specificity of the hemagglutinin from an H5N1 influenza virus. *Science (New York, N.Y.)*. **2006**, *312*, 404–410.

[31] Tang, G.; Qiu, Z.; Lin, X.; Li, W.; Zhu, L.; Li, S.; Li, H.; Wang, L.; Chen, L.; Wu, J. Z.; Yang, W. Discovery of novel 1-phenyl-cycloalkane carbamides as potent and selective influenza fusion inhibitors. *Bioorganic & Medicinal Chemistry Letters*. **2010**, *20*, 3507–3510.

[32] Portela, A.; Digard, P. The influenza virus nucleoprotein: a multifunctional RNA-binding protein pivotal to virus replication. *The Journal of General Virology*. **2002**, *83*, 723–734.

[33] Du, J.; Cross, T. A.; Zhou, H.-X. Recent progress in structure-based anti-influenza drug design. *Drug Discovery Today*. **2012**, *17*, 1111–1120.

[34] Sharma, M.; Yi, M.; Dong, H.; Qin, H.; Peterson, E.; Busath, D. D.; Zhou, H.-X.; Cross, T. A. Insight into the mechanism of the influenza A proton channel from a structure in a lipid bilayer. *Science (New York, N.Y.)*. **2010**, *330*, 509–512.

[35] Hale, B. G.; Randall, R. E.; Ortín, J.; Jackson, D. The multifunctional NS1 protein of influenza A viruses. *The Journal of General Virology*. **2008**, *89*, 2359–2376.

[36] Steinhauer, D. A.; Skehel, J. J. Genetics of influenza viruses. *Annual Review of Genetics*. **2002**, *36*, 305–332.

[37] Krug, R. M.; Broni, B. A.; Bouloy, M. Are the 5' ends of influenza viral mRNAs synthesized in vivo donated by host mRNAs?. *Cell*. **1979**, *18*, 329–334.

[38] He, X.; Zhou, J.; Bartlam, M.; Zhang, R.; Ma, J.; Lou, Z.; Li, X.; Li, J.; Joachimiak, A.; Zeng, Z.; Ge, R.; Rao, Z.; Liu, Y. Crystal structure of the polymerase PA(C)-PB1(N) complex from an avian influenza H5N1 virus. *Nature*. **2008**, *454*, 1123–1126.

[39] Sugiyama, K.; Obayashi, E.; Kawaguchi, A.; Suzuki, Y.; Tame, J. R. H.; Nagata, K.; Park, S.-Y. Structural insight into the essential PB1-PB2 subunit contact of the influenza virus RNA polymerase. *The EMBO journal*. **2009**, *28*, 1803–1811.

[40] Krug, R. M.; Aramini, J. M. Emerging antiviral targets for influenza A virus. *Trends in Pharmacological Sciences*. **2009**, *30*, 269–277.

[41] von Itzstein, M. The war against influenza: discovery and development of sialidase inhibitors. *Nature Reviews. Drug Discovery*. **2007**, *6*, 967–974.

[42] Steinhauer, D. A. Role of hemagglutinin cleavage for the pathogenicity of influenza virus. *Virology*. **1999**, *258*, 1–20.

[43] Stegmann, T. Membrane fusion mechanisms: the influenza hemagglutinin paradigm and its implications for intracellular fusion. *Traffic (Copenhagen, Denmark)*. **2000**, *1*, 598–604.

[44] Sieczkarski, S. B.; Whittaker, G. R. Viral entry. *Current Topics in Microbiology and Immunology*. **2005**, *285*, 1–23.

[45] Cros, J. F.; Palese, P. Trafficking of viral genomic RNA into and out of the nucleus: influenza, Thogoto and Borna disease viruses. *Virus Research*. **2003**, *95*, 3–12.

[46] Palese, P.; Shaw, M. L. Orthomyxoviridae: The Viruses and their Replication. *Fields Virology. Philadelphia: Lippincott Williams & Wilkins*. **2007**.

[47] Fujii, Y.; Goto, H.; Watanabe, T.; Yoshida, T.; Kawaoka, Y. Selective incorporation of influenza virus RNA segments into virions. *Proceedings of the National Academy of Sciences of the United States of America*. **2003**, *100*, 2002–2007.

[48] Van Regenmortel, M. H. Antigenicity and immunogenicity of synthetic peptides. *Biologicals: Journal of the International Association of Biological Standardization*. **2001**, *29*, 209–213.

[49] Potter, C. W.; Oxford, J. S. Determinants of immunity to influenza infection in man. *British Medical Bulletin*. **1979**, *35*, 69–75.

[50] Smith, F. I.; Palese, P. Variation in Influenza Virus Genes. *The Influenza Viruses*. **1989**, 319–359.

[51] Treanor, J. Influenza vaccine—outmaneuvering antigenic shift and drift. *New England Journal of Medicine*. **2004**, *350*, 218–220.

[52] Lam, T. T.-Y.; Zhu, H.; Wang, J.; Smith, D. K.; Holmes, E. C.; Webster, R. G.; Webby, R.; Peiris, J. M.; Guan, Y. Reassortment events among swine influenza A viruses in China: implications for the origin of the 2009 influenza pandemic. *Journal of Virology*. **2011**, *85*, 10279–10285.

[53] Gong, J.; Xu, W.; Zhang, J. Structure and functions of influenza virus neuraminidase. *Current medicinal chemistry*. **2007**, *14*, 113–122.

[54] van Riel, D.; Munster, V. J.; de Wit, E.; Rimmelzwaan, G. F.; Fouchier, R. A. M.; Osterhaus, A. D. M. E.; Kuiken, T. H5N1 Virus Attachment to Lower Respiratory Tract. *Science (New York, N.Y.)*. **2006**, *312*, 399.

[55] Clayville, L. R. Influenza update: a review of currently available vaccines. *P & T: A Peer-Reviewed Journal for Formulary Management*. **2011**, *36*, 659–684.

[56] Hannoun, C.; Megas, F.; Piercy, J. Immunogenicity and protective efficacy of influenza vaccination. *Virus Research*. **2004**, *103*, 133–138.

[57] Brydak, L. B.; Machala, M. Humoral immune response to influenza vaccination in patients from high risk groups. *Drugs*. **2000**, *60*, 35–53.

[58] Beigel, J. Antivirals compounds in the pipeline to tackle H1N1 Influenza infection. *Drugs of the Future*. **2010**, *35*, 385.

[59] Centers for Disease Control and Prevention (CDC). High levels of adamantane resistance among influenza A (H3N2) viruses and interim guidelines for use of antiviral agents–United States, 2005-06 influenza season. *MMWR. Morbidity and mortality weekly report*. **2006**, *55*, 44–46.

[60] Garman, E.; Laver, G. The structure, function, and inhibition of influenza virus neuraminidase. *Viral Membrane Proteins: Structure, Function, and Drug Design*. **2005**, 247–267.

[61] Matrosovich, M. N.; Matrosovich, T. Y.; Gray, T.; Roberts, N. A.; Klenk, H.-D. Neuraminidase is important for the initiation of influenza virus infection in human airway epithelium. *Journal of Virology*. **2004**, *78*, 12665–12667.

[62] Muñoz-Barroso, I.; García-Sastre, A.; Villar, E.; Manuguerra, J. C.; Hannoun, C.; Cabezas, J. A. Increased influenza A virus sialidase activity with N-acetyl-9-O-acetylneuraminic acid-containing substrates resulting from influenza C virus O-acetylesterase action. *Virus Research*. **1992**, *25*, 145–153.

[63] *Protein Data Bank*. http://www.rcsb.org/pdb/explore.do?structureId=1w21; cited: January 30th 2015.

[64] Air, G. M. Influenza neuraminidase. *Influenza and Other Respiratory Viruses*. **2012**, *6*, 245–256.

[65] Laver, W. G. Crystallization and peptide maps of neuraminidase "heads" from H2N2 and H3N2 influenza virus strains. *Virology*. **1978**, *86*, 78–87.

[66] Sun, X.; Li, Q.; Wu, Y.; Wang, M.; Liu, Y.; Qi, J.; Vavricka, C. J.; Gao, G. F. Structure of influenza virus N7: the last piece of the neuraminidase "jigsaw" puzzle. *Journal of Virology*. **2014**, *88*, 9197–9207.

[67] Leang, S.-K.; Kwok, S.; Sullivan, S. G.; Maurer-Stroh, S.; Kelso, A.; Barr, I. G.; Hurt, A. C. Peramivir and laninamivir susceptibility of circulating influenza A and B viruses. *Influenza and Other Respiratory Viruses*. **2014**, *8*, 135–139.

[68] Woods, J. M.; Bethell, R. C.; Coates, J. A.; Healy, N.; Hiscox, S. A.; Pearson, B. A.; Ryan, D. M.; Ticehurst, J.; Tilling, J.; Walcott, S. M. 4-Guanidino-2,4-dideoxy-2,3-dehydro-N-acetylneuraminic acid is a highly effective inhibitor both of the sialidase (neuraminidase) and of growth of a wide range of influenza A and B viruses in vitro. *Antimicrobial Agents and Chemotherapy*. **1993**, *37*, 1473–1479.

[69] Kim, C. U.; Lew, W.; Williams, M. A.; Liu, H.; Zhang, L.; Swaminathan, S.; Bischofberger, N.; Chen, M. S.; Mendel, D. B.; Tai, C. Y.; Laver, W. G.; Stevens, R. C. Influenza neuraminidase inhibitors possessing a novel hydrophobic interaction in the enzyme active site: design, synthesis, and structural analysis of carbocyclic sialic acid analogues with potent anti-influenza activity. *Journal of the American Chemical Society*. **1997**, *119*, 681–690.

[70] Yongkiettrakul, S.; Nivitchanyong, T.; Pannengpetch, S.; Wanitchang, A.; Jongkaewwattana, A.; Srimanote, P. Neuraminidase amino acids 149 and 347 determine the infectivity and oseltamivir sensitivity of pandemic influenza A/H1N1 (2009) and avian influenza A/H5N1. *Virus Research*. **2013**, *175*, 128–133.

[71] Koyama, K.; Takahashi, M.; Oitate, M.; Nakai, N.; Takakusa, H.; Miura, S.-i.; Okazaki, O. CS-8958, a prodrug of the novel neuraminidase inhibitor R-125489, demonstrates a favorable long-retention profile in the mouse respiratory tract. *Antimicrobial Agents and Chemotherapy*. **2009**, *53*, 4845–4851.

[72] Ishizuka, H.; Yoshiba, S.; Okabe, H.; Yoshihara, K. Clinical pharmacokinetics of laninamivir, a novel long-acting neuraminidase inhibitor, after single and multiple inhaled doses of its prodrug, CS-8958, in healthy male volunteers. *Journal of Clinical Pharmacology*. **2010**, *50*, 1319–1329.

[73] Brown, A. N.; Bulitta, J. B.; McSharry, J. J.; Weng, Q.; Adams, J. R.; Kulawy, R.; Drusano, G. L. Effect of half-life on the pharmacodynamic index of zanamivir against influenza virus delineated by a mathematical model. *Antimicrobial Agents and Chemotherapy*. **2011**, *55*, 1747–1753.

[74] Ikematsu, H.; Kawai, N.; Iwaki, N.; Kashiwagi, S. In vitro neuraminidase inhibitory activity of four neuraminidase inhibitors against clinical isolates of influenza virus in the Japanese 2012-2013 season. *Journal of Infection and Chemotherapy: Official Journal of the Japan Society of Chemotherapy*. **2015**, *21*, 39–42.

[75] Babu, Y. S.; Chand, P.; Bantia, S.; Kotian, P.; Dehghani, A.; El-Kattan, Y.; Lin, T. H.; Hutchison, T. L.; Elliott, A. J.; Parker, C. D.; Ananth, S. L.; Horn, L. L.; Laver, G. W.; Montgomery, J. A. BCX-1812 (RWJ-270201): discovery of a novel, highly potent, orally active, and selective influenza neuraminidase inhibitor through structure-based drug design. *Journal of Medicinal Chemistry*. **2000**, *43*, 3482–3486.

[76] Birnkrant, D.; Cox, E. The Emergency Use Authorization of peramivir for treatment of 2009 H1N1 influenza. *The New England Journal of Medicine*. **2009**, *361*, 2204–2207.

[77] Shie, J.-J.; Fang, J.-M.; Wong, C.-H. A Concise and Flexible Synthesis of the Potent Anti-Influenza Agents Tamiflu and Tamiphosphor. *Angewandte Chemie International Edition*. **2008**, *47*, 5788–5791.

[78] Shie, J.-J.; Fang, J.-M. Phosphonate Congeners of Oseltamivir and Zanamivir as Effective Anti-influenza Drugs: Design, Synthesis and Biological Activity. *Journal of the Chinese Chemical Society*. **2014**, *61*, 127–141.

[79] Su, C.-Y.; Wang, S.-Y.; Shie, J.-J.; Jeng, K.-S.; Temperton, N. J.; Fang, J.-M.; Wong, C.-H.; Cheng, Y.-S. E. In vitro evaluation of neuraminidase inhibitors using the neuraminidase-dependent release assay of hemagglutinin-pseudotyped viruses. *Antiviral Research*. **2008**, *79*, 199–205.

[80] Boivin, G. Detection and management of antiviral resistance for influenza viruses. *Influenza and Other Respiratory Viruses*. **2013**, *7*, 18–23.

[81] Ison, M. G. Antivirals and resistance: influenza virus. *Current Opinion in Virology*. **2011**, *1*, 563–573.

[82] Shiraishi, K.; Mitamura, K.; Sakai-Tagawa, Y.; Goto, H.; Sugaya, N.; Kawaoka, Y. High frequency of resistant viruses harboring different mutations in amantadine-treated children with influenza. *The Journal of Infectious Diseases*. **2003**, *188*, 57–61.

[83] Mishin, V. P.; Hayden, F. G.; Gubareva, L. V. Susceptibilities of antiviral-resistant influenza viruses to novel neuraminidase inhibitors. *Antimicrobial Agents and Chemotherapy*. **2005**, *49*, 4515–4520.

[84] McKimm-Breschkin, J. L. Influenza neuraminidase inhibitors: antiviral action and mechanisms of resistance. *Influenza and Other Respiratory Viruses*. **2013**, *7 Suppl 1*, 25–36.

[85] Abed, Y.; Baz, M.; Boivin, G. Impact of neuraminidase mutations conferring influenza resistance to neuraminidase inhibitors in the N1 and N2 genetic backgrounds. *Antiviral Therapy*. **2006**, *11*, 971–976.

[86] Das, K.; Aramini, J. M.; Ma, L.-C.; Krug, R. M.; Arnold, E. Structures of influenza A proteins and insights into antiviral drug targets. *Nature Structural & Molecular Biology*. **2010**, *17*, 530–538.

[87] Russell, R. J.; Haire, L. F.; Stevens, D. J.; Collins, P. J.; Lin, Y. P.; Blackburn, G. M.; Hay, A. J.; Gamblin, S. J.; Skehel, J. J. The structure of H5N1 avian influenza neuraminidase suggests new opportunities for drug design. *Nature*. **2006**, *443*, 45–49.

[88] Collins, P. J.; Haire, L. F.; Lin, Y. P.; Liu, J.; Russell, R. J.; Walker, P. A.; Skehel, J. J.; Martin, S. R.; Hay, A. J.; Gamblin, S. J. Crystal structures of oseltamivir-resistant influenza virus neuraminidase mutants. *Nature*. **2008**, *453*, 1258–1261.

[89] Wu, Y.; Bi, Y.; Vavricka, C. J.; Sun, X.; Zhang, Y.; Gao, F.; Zhao, M.; Xiao, H.; Qin, C.; He, J.; Liu, W.; Yan, J.; Qi, J.; Gao, G. F. Characterization of two distinct neuraminidases from avian-origin human-infecting H7N9 influenza viruses. *Cell Research*. **2013**, *23*, 1347–1355.

[90] Nitsch-Osuch, A.; Brydak, L. B. Influenza viruses resistant to neuraminidase inhibitors. *Acta Biochimica Polonica*. **2014**, *61*, 505–508.

[91] Samson, M.; Pizzorno, A.; Abed, Y.; Boivin, G. Influenza virus resistance to neuraminidase inhibitors. *Antiviral Research*. **2013**, *98*, 174–185.

[92] Fiore, A. E.; Fry, A.; Shay, D.; Gubareva, L.; Bresee, J. S.; Uyeki, T. M. Antiviral agents for the treatment and chemoprophylaxis of influenza: recommendations of the Advisory Committee on Immunization Practices (ACIP). **2011**.

[93] Spanakis, N.; Pitiriga, V.; Gennimata, V.; Tsakris, A. A review of neuraminidase inhibitor susceptibility in influenza strains. *Expert Review of Anti-Infective Therapy*. **2014**, *12*, 1325–1336.

[94] Husain, M. Avian influenza A (H7N9) virus infection in humans: epidemiology, evolution, and pathogenesis. *Infection, Genetics and Evolution: Journal of Molecular Epidemiology and Evolutionary Genetics in Infectious Diseases*. **2014**, *28*, 304–312.

[95] Fouchier, R. A. M.; Schneeberger, P. M.; Rozendaal, F. W.; Broekman, J. M.; Kemink, S. A. G.; Munster, V.; Kuiken, T.; Rimmelzwaan, G. F.; Schutten, M.; Van Doornum, G. J. J.; Koch, G.; Bosman, A.; Koopmans, M.; Osterhaus, A. D. M. E. Avian influenza A virus (H7N7) associated with human conjunctivitis and a fatal case of acute respiratory distress syndrome. *Proceedings of the National Academy of Sciences of the United States of America*. **2004**, *101*, 1356–1361.

[96] Hirst, M.; Astell, C. R.; Griffith, M.; Coughlin, S. M.; Moksa, M.; Zeng, T.; Smailus, D. E.; Holt, R. A.; Jones, S.; Marra, M. A.; Petric, M.; Krajden, M.; Lawrence, D.; Mak, A.; Chow, R.; Skowronski, D. M.; Tweed, S. A.; Goh, S.; Brunham, R. C.; Robinson, J.; Bowes, V.; Sojonky, K.; Byrne, S. K.; Li, Y.; Kobasa, D.; Booth, T.; Paetzel, M. Novel Avian Influenza H7N3 Strain Outbreak, British Columbia. *Emerging Infectious Diseases*. **2004**, *10*, 2192–2195.

[97] Kalthoff, D.; Bogs, J.; Harder, T.; Grund, C.; Pohlmann, A.; Beer, M.; Hoffmann, B. Nucleic acid-based detection of influenza A virus subtypes H7 and N9 with a special emphasis on the avian H7N9 virus. *Euro Surveillance: Bulletin Européen Sur Les Maladies Transmissibles = European Communicable Disease Bulletin*. **2014**, *19*.

[98] Shen, Y.; Lu, H. Human infection with avian influenza A(H7N9) virus in Shanghai: current status and future trends. *Chinese Medical Journal*. **2014**, *127*, 1973–1976.

[99] Chin, A. W. H.; Mok, C. K. P.; Zhu, H.; Guan, Y.; Peiris, J. S. M.; Poon, L. L. M. Use of fractional factorial design to study the compatibility of viral ribonucleoprotein gene segments of human H7N9 virus and circulating human influenza subtypes. *Influenza and Other Respiratory Viruses*. **2014**, *8*, 580–584.

[100] *January 2014, WHO H7N9 report*. `http://www.who.int/influenza/human_animal_interface/influenza_h7n9/ReportH7N9Number_20140130.pdf?ua=1`; cited: February 1st 2015.

[101] *July 2014, WHO H7N9 report*. `http://www.who.int/influenza/human_animal_interface/influenza_h7n9/18_reportwebh7n9number_20140714.pdf?ua=1`; cited: February 1st 2015.

[102] Watanabe, T.; Watanabe, S.; Maher, E. A.; Neumann, G.; Kawaoka, Y. Pandemic potential of avian influenza A (H7N9) viruses. *Trends in Microbiology*. **2014**, *22*, 623–631.

[103] *Flu database used for sequence alignment of mentioned influenza strains*. `http://www.fludb.org/brc/home.spg?decorator=influenza`; cited: February 1st 2015.

[104] Varghese, J. N.; Smith, P. W.; Sollis, S. L.; Blick, T. J.; Sahasrabudhe, A.; McKimm-Breschkin, J. L.; Colman, P. M. Drug design against a shifting target: a structural basis for resistance to inhibitors in a variant of influenza virus neuraminidase. *Structure (London, England: 1993)*. **1998**, *6*, 735–746.

[105] Yen, H.-L.; Herlocher, L. M.; Hoffmann, E.; Matrosovich, M. N.; Monto, A. S.; Webster, R. G.; Govorkova, E. A. Neuraminidase inhibitor-resistant influenza viruses may differ substantially in fitness and transmissibility. *Antimicrobial Agents and Chemotherapy*. **2005**, *49*, 4075–4084.

[106] Carr, J.; Ives, J.; Kelly, L.; Lambkin, R.; Oxford, J.; Mendel, D.; Tai, L.; Roberts, N. Influenza virus carrying neuraminidase with reduced sensitivity to oseltamivir carboxylate has altered properties in vitro and is compromised for infectivity and replicative ability in vivo. *Antiviral Research*. **2002**, *54*, 79–88.

[107] *Precision Plus Protein; All Blue Standards*. `http://www.bio-rad.com/en-us/sku/161-0373edu-precision-plus-protein-all-blue-standards`; cited: April 28th 2015.

Svoluji k zapůjčení této práce pro studijní účely a prosím, aby byla řádně vedena evidence vypůjčovatelů.

Jméno a příjmení, adresa	Číslo OP	Datum vypůjčení	Poznámka